PB87-133096

Pilot-Scale Evaluation of Top-Inlet and Advanced Electrostatic Filtration

Research Triangle Inst.
Research Triangle Park, NC

Prepared for

Environmental Protection Agency
Research Triangle Park, NC

Nov 86

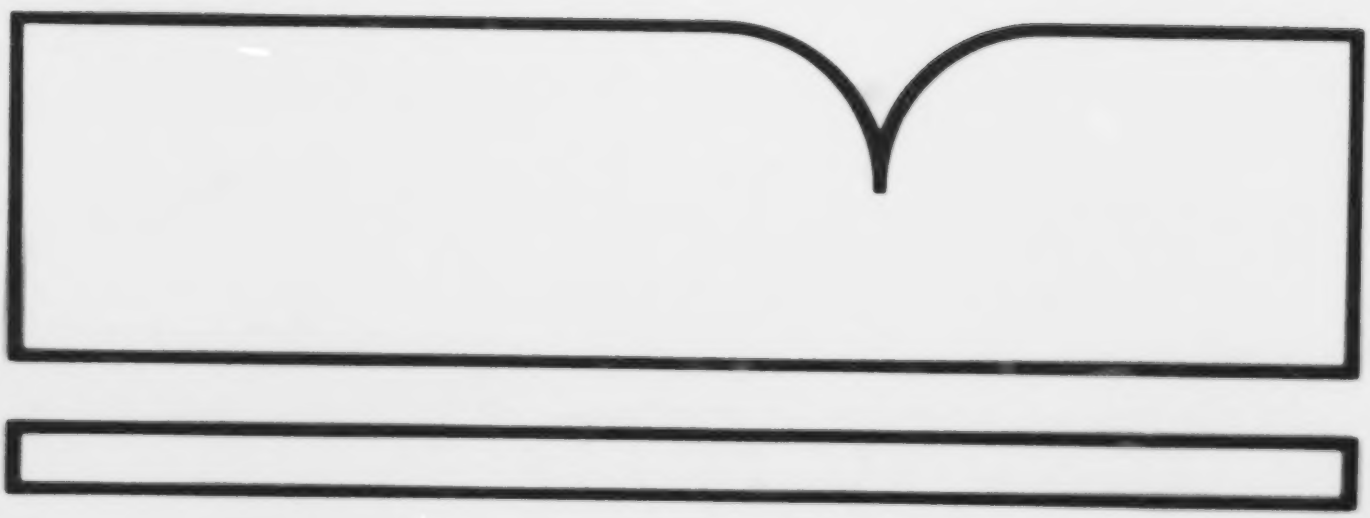

U.S. Department of Commerce
National Technical Information Service
NTIS

PB87-133096

EPA/600/7-86/042
November 1986

PILOT-SCALE EVALUATION OF TOP-INLET AND ADVANCED ELECTROSTATIC FILTRATION

by

A. S. Viner
Research Triangle Institute
P.O. Box 12194
Research Triangle Park, North Carolina 27709

G.P. Greiner, D.F. Furlong, and R.G. Hurst
ETS, Inc.
3140 Chaparral Drive, S.W.
Roanoke, Virginia 24018

EPA Cooperative Agreement CR810152

Project Officer
L.S. Hovis
Air and Energy Engineering Research Laboratory
U.S. Environmental Protection Agency
Research Triangle Park, North Carolina 27711

Prepared for

U.S. ENVIRONMENTAL PROTECTION AGENCY
OFFICE OF RESEARCH AND DEVELOPMENT
WASHINGTON, D.C. 20460

AIR AND ENERGY ENGINEERING RESEARCH LABORATORY
OFFICE OF RESEARCH AND DEVELOPMENT
U.S. ENVIRONMENTAL PROTECTION AGENCY
RESEARCH TRIANGLE PARK, NC 27711

REPRODUCED BY
U.S. DEPARTMENT OF COMMERCE
NATIONAL TECHNICAL
INFORMATION SERVICE
SPRINGFIELD, VA. 22161

TECHNICAL REPORT DATA
(Please read Instructions on the reverse before completing)

1. REPORT NO. EPA/600/7-86/042	2.
3. RECIPIENT'S ACCESSION NO. PB87 133096/AS	
4. TITLE AND SUBTITLE Pilot-scale Evaluation of Top-inlet and Advanced Electrostatic Filtration	5. REPORT DATE November 1986
	6. PERFORMING ORGANIZATION CODE
7. AUTHOR(S) A. S. Viner (RTI); G. P. Greiner, D. F. Furlong, and R. G. Hurst (ETS)*	8. PERFORMING ORGANIZATION REPORT NO. 47U-2513-7
9. PERFORMING ORGANIZATION NAME AND ADDRESS Research Triangle Institute, P. O. Box 12194, Research Triangle Park, North Carolina 27709	10. PROGRAM ELEMENT NO.
	11. CONTRACT/GRANT NO. CR810152
12. SPONSORING AGENCY NAME AND ADDRESS EPA, Office of Research and Development, Air and Energy Engineering Research Laboratory, Research Triangle Park, NC 27711	13. TYPE OF REPORT AND PERIOD COVERED Final; 2-9/85
	14. SPONSORING AGENCY CODE EPA/600/13

15. SUPPLEMENTARY NOTES AEERL project officer is Louis S. Hovis, Mail Drop 61, 919/541-3374. (*) ETS, Inc., 3140 Chaparral Drive, SW, Roanoke, VA 24018.

16. ABSTRACT The report gives results of an evaluation of Advanced Electrostatic Augmentation of Fabric Filtration (ESFF) on a slipstream from a stoker-fired boiler. Advanced ESFF, with its characteristic high-voltage center-wire electrode, was compared with conventional filter bags in the same baghouse using calibrated flow orifices. The advantage of advanced ESFF was demonstrated by consistently higher gas flow rates in the bags with the corona producing electrodes. Analysis of the data showed that the specific resistance of an electrostatically enhanced filter was 70% less than that of a conventional bag. An economic analysis showed a capital cost savings of 26% with advanced ESFF based on doubling the air/cloth ratio for advanced ESFF. In a second test, the feasibility of using top-inlet filtration on stoker fly ash was established. No definitive comparison with conventional bottom-inlet filtration could be made in the allotted test period.

17. KEY WORDS AND DOCUMENT ANALYSIS

a. DESCRIPTORS	b. IDENTIFIERS/OPEN ENDED TERMS	c. COSATI Field/Group
Pollution, Flue Gases	Pollution Control	13B
Filtration, Boilers	Stationary Sources	07D, 13A
Electrostatics, Fly Ash	Electrostatic Filtration	20C
Fabrics, Particles	Fabric Filters	11E, 14G
Coal Combustion	Particulate	21D, 21B

18. DISTRIBUTION STATEMENT Release to Public	19. SECURITY CLASS (This Report) Unclassified	21. NO. OF PAGES 69
	20. SECURITY CLASS (This page) Unclassified	22. PRICE

EPA Form 2220-1 (9-73)

NOTICE

This document has been reviewed in accordance with U.S. Environmental Protection Agency policy and approved for publication. Mention of trade names or commercial products does not constitute endorsement or recommendation for use.

ABSTRACT

Two new fly ash filtration strategies were evaluated at pilot scale: top-inlet filtration and advanced electrostatic stimulation of fabric filtration (advanced ESFF). Two identical compartments filtered ash-laden air taken from a slip stream of a stoker-fired boiler. In one compartment there were three conventional, reverse air-cleaned, bottom-inlet bags and three bags with electrodes hung from the center of the bag cap. A high voltage (20 - 35 kV, 1 - 2 mA) maintained on the electrode established an electric field between the center electrode and the surface of the bag. All bags in this compartment were fitted with calibrated flow orifices to measure the flow into the bags. The second compartment contained bags that were opened at each end and attached to both an upper and lower tubesheet. Gas entered from the top of the compartment and was removed through a duct in the side wall. Data collection was automated by a data logger and an attached microcomputer. Long-distance communication with the computer permitted daily analysis of the data in the absense of an onsite operator.

The feasibility of the advanced ESFF concept was demonstrated by consistently higher flows through the bags with the high-voltage electrodes. Analysis of the data showed the specific resistance of an electrostatically augmented filter to be 70 percent below that of a conventional filter. There was not sufficient data to draw a conclusion about the impact of the electric field on the residual drag of the bags. Problems with cleaning hardware limited the amount of valid data collected on the top-inlet compartment. Few conclusions can be drawn from that information.

An economic analysis of the application of advanced ESFF to industrial-scale boilers shows that the capital cost of an advanced ESFF baghouse designed with an air-to-cloth ratio of 1.22 m/min (4 ft/min) would be 26 percent less than the cost of a conventional baghouse designed for 0.61 m/min (2 ft/min). Similar savings in operating and maintenance costs can be expected.

TABLE OF CONTENTS

Section		Page
1	Introduction	1
2	Pilot Plant Design	8
3	Data Acquisition and Analysis	14
	Data Acquisition System	14
	Data Analysis	15
4	Results	18
	Bottom-Inlet Compartment	18
	Top-Inlet Compartment	36
5	Economic Analysis of Advanced ESFF	41
6	Discussion	47
7	Conclusions and Recommendations	52
8	References	54
Appendix	Data Quality Assessment	55

FIGURES

Number		Page
1	A typical reverse-air-cleaned baghouse	2
2	The center-wire configuration of ESFF	5
3	A conceptual design of a top-inlet baghouse	6
4	Schematic of Cherry Point pilot plant	9
5	A prototype electrode design for implementation of advanced ESFF	11
6	Power supply control circuit	13
7	Average air-to-cloth ratio for each bag in bottom-inlet compartments	20
8	IBFM pressure drop curves: August 29 through August 31	23
9	Individual bag-flow data from ESFF pilot plant	24
10	Tubesheet pressure drop for top-inlet and bottom-inlet compartments: August 29 through August 31	25
11	Drag correlation for bag number 1 (ESFF)	27
12	Drag correlation for bag number 2 (conventional)	27
13	Summary of the specific resistance for each bag in the bottom-inlet compartment	28
14	Individual bag-flow data (cycle average air-to-cloth ratio) when the voltage was switched	30
15	The pressure-drop ratio of specific resistances	31
16	Residual drag results (drag at the beginning of the filtration cycle)	33
17	Average electrode voltage for each cycle	34
18	Average current output from the power supply	35
19	Residual drag for conventional bags (bottom inlet) versus top-inlet bags	38
20	Specific resistance for conventional bags (bottom inlet) versus top-inlet bags	40

FIGURES (continued)

Number		Page
21	ESFF capital cost savings	43
22	Annual ESFF operating and maintenance cost savings	46
23	An improved electrode design	49

TABLES

Number		Page
1	Particulate Loading Data	22
2	Advanced Baghouse Capital Cost Comparison	42
3	Annual Operating Cost Comparison	45
4	Summary of Precision, Accuracy, and Completeness Objectives	57
5	Precision and Accuracy Data	58

Acknowledgments

The authors would like to acknowledge the cooperation and assistance received from personnel of the Cherry Point Marine Corps Air Station. Also appreciated was the rapid response of National Filter Media, Inc., in modifying several filter bags.

SECTION 1

INTRODUCTION

The adoption of strict air pollution laws in the United States has prompted the search for efficient, economical pollution control devices. In the electric utility industry, electrostatic precipitators have been the traditional method of collecting the fly ash that results from burning coal. These precipitators generally worked well and allowed the utilities to meet the emissions requirements. However, as more and more generators began burning western low-sulfur coal, the size and cost of precipitators required to meet the emissions standards increased. In search of an alternative, the utilities turned to fabric filters (also known as baghouses) because of their high efficiency and competitive costs.

A conceptual design of a baghouse is shown in Figure 1. Dust-laden air enters the baghouse compartment from below and travels up through a tubesheet into the fabric bags. When the air passes through the fabric, the dust is retained on the surface of the bag. In this way, a fabric filter is similar to a household vacuum cleaner. Baghouses have proven very popular with the utility industry since the first installation in the 1970s. Since then, the search for methods to lower costs and maintain high efficiency has continued.

In general, the high efficiency of a fabric filter is inherent in the design. As a dust layer builds up on the surface of the fabric, the number of direct pathways that an airborne particle can follow from the dirty side to the clean side of the fabric decreases. Eventually, few, if any, direct pathways for dust penetration remain. At this point, the dust emissions are very low, resulting mostly from the slow seepage of dust through the fabric. As the dust layer builds up, the amount of energy required to draw air through the dust layer and fabric increases. This energy requirement is expressed as the pressure differential across the dust/fabric layer at a given air-flow rate. As pressure loss grows, the cost of drawing the air through the filter increases. Eventually, the air flow is stopped so that the bag can be cleaned, either by shaking or reversing the flow with clean air.

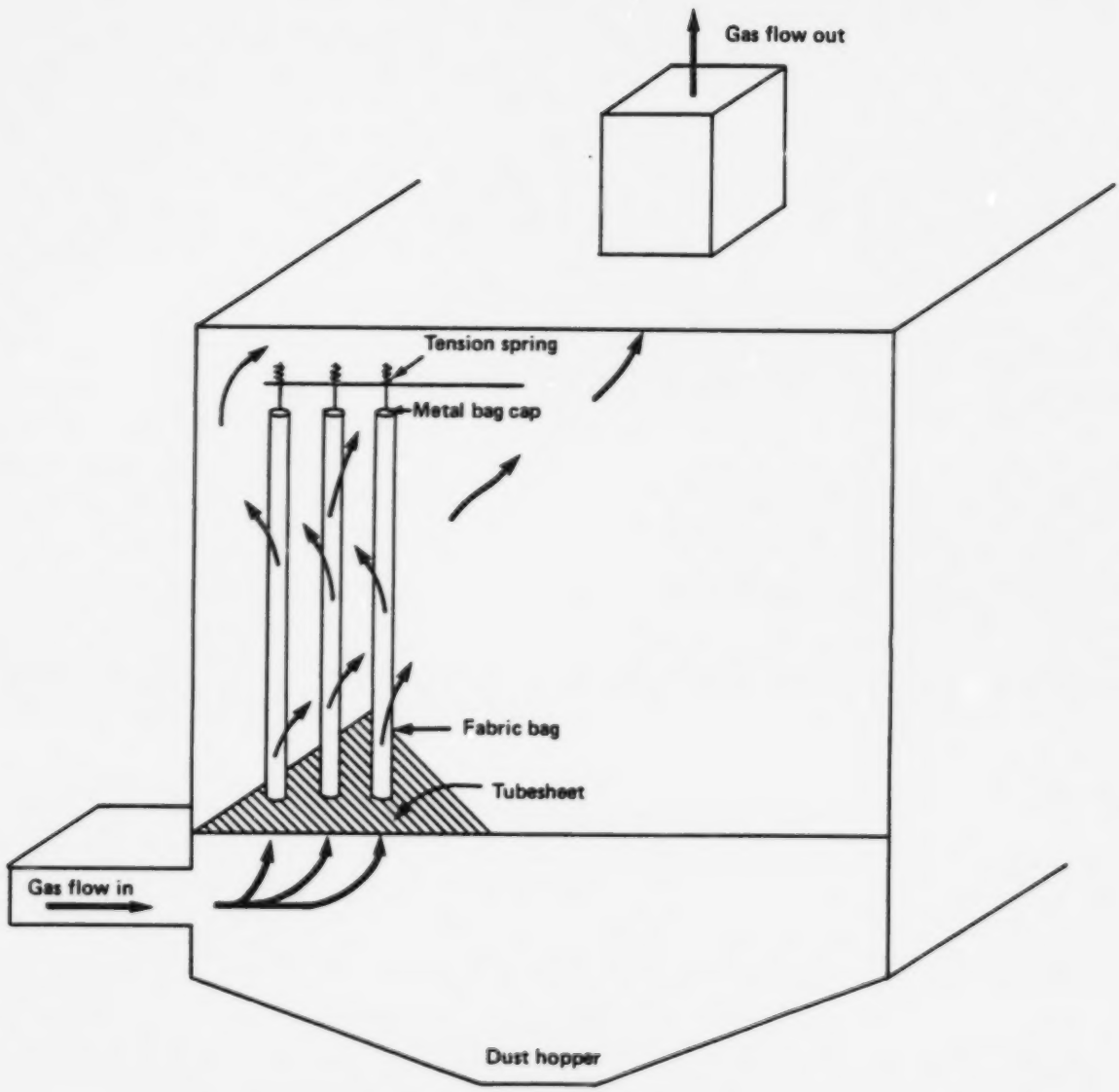

Figure 1. A typical reverse-air-cleaned baghouse.

Fan cost considerations dictate that the pressure loss must remain within a certain range. Also, the rate at which pressure loss grows has important implications for other baghouse equipment. In general, it is better to have a slow rate of pressure loss. Because the pressure loss is related to the amount of dust on the fabric, the way to keep pressure loss low and prevent it from increasing rapidly is to ensure a slow rate of dust deposition. This implies that the amount of fabric area available for dust deposition is an important design parameter. The ratio of the air-flow rate to the filter area is called the air-to-cloth ratio or face velocity. The problem encountered in baghouse design is in specifying the highest possible air-to-cloth ratio (to minimize the overall size and cost) while ensuring that pressure loss limitations are not exceeded.

Many methods have been proposed to lower this dust-cake pressure drop, and most of them are based on the concept of altering the structure of the dust cake to permit easier gas passage while maintaining high collection efficiency. Two such methods are the focus of this report: electric field enhancement and top-inlet design.

It is well known that the dust particles emitted from a coal-fired boiler have a static charge. An early idea in baghouse research focused on increasing this natural charge on the particles by placing a corona precharger at the entrance to a filter bag. This design is employed in the APITRON collector and has been evaluated by Felix and McCain (1). Another idea for lowering the pressure drop across a filter is to put electrodes of opposite polarity on the fabric surface and generate an electric field parallel to the fabric. This idea was explored extensively in the laboratory by Miller et al. (2) and in a pilot plant by VanOsdell et al. (3, 4) and Chambers (5). This latter method of electrical enhancement is known as electrostatic stimulation of fabric filtration (ESFF). Although these methods have been proven successful in reducing the pressure drop, they have yet to gain acceptance in the filter-using community. Two reasons for this are that the hardware required to implement the technology can be complicated and the cost savings projected for these technologies are not significant enough to overcome the natural disdain for "unproven" methods.

Recently, a new method of electric field enhancement was investigated in the laboratories of the U.S. Environmental Protection Agency (EPA). The new method requires the placement of an electrode in the center of the filter bag (Figure 2). When a high voltage is imposed on the electrode, an electric field is established between the electrode and the dust/fabric surface. The presence of the electric field alters the dust deposition pattern and the structure of the dust cake, resulting in a reduction in the pressure drop across the bag. Laboratory results showed that this design reduced the rate of pressure drop increase by 90 percent; this improvement is much better than that offered by either the APITRON collector or the parallel field collector. In addition, the hardware is simpler than other collectors. This new design has been termed "advanced" ESFF.

Although researchers have found that electrostatic enhancement lowers pressure drop, all of the proposed methods have the disadvantage of increasing the amount of hardware required. The feeling remains that more can and should be done in designing and operating standard filters to optimize performance.

Jensen (6) proposed the use of the top-inlet design to improve performance. In the standard baghouse design--where dirty gas must enter the bag from the bottom and flow upwards--large particles either fall out of the gas into the hopper without reaching the bag or are deposited on the lower portion of the bag. Jensen suggested that the bottom-inlet design may allow for an elutriation effect where the average particle size deposited on a bag decreases with distance from the bottom inlet. Jensen also suggested that the dust-cake resistance increases as the mean particle size decreases, producing an increase in flow resistance with the distance up the bag. Based on this hypothesis, Jensen recommends that a bag should be open at both the top and the bottom, with the dust-laden gas being introduced from the top. This concept is illustrated schematically in Figure 3. With a top-inlet design, the large particles would be retained in the gas and distributed more evenly along the length of the bag. This would make the dust-cake resistance lower and more uniform than that of a bottom-inlet bag. Greiner et al. (7) reported favorable results for a top-inlet pilot plant using short bags. To date, there have been no studies of top-inlet filters using full-size bags.

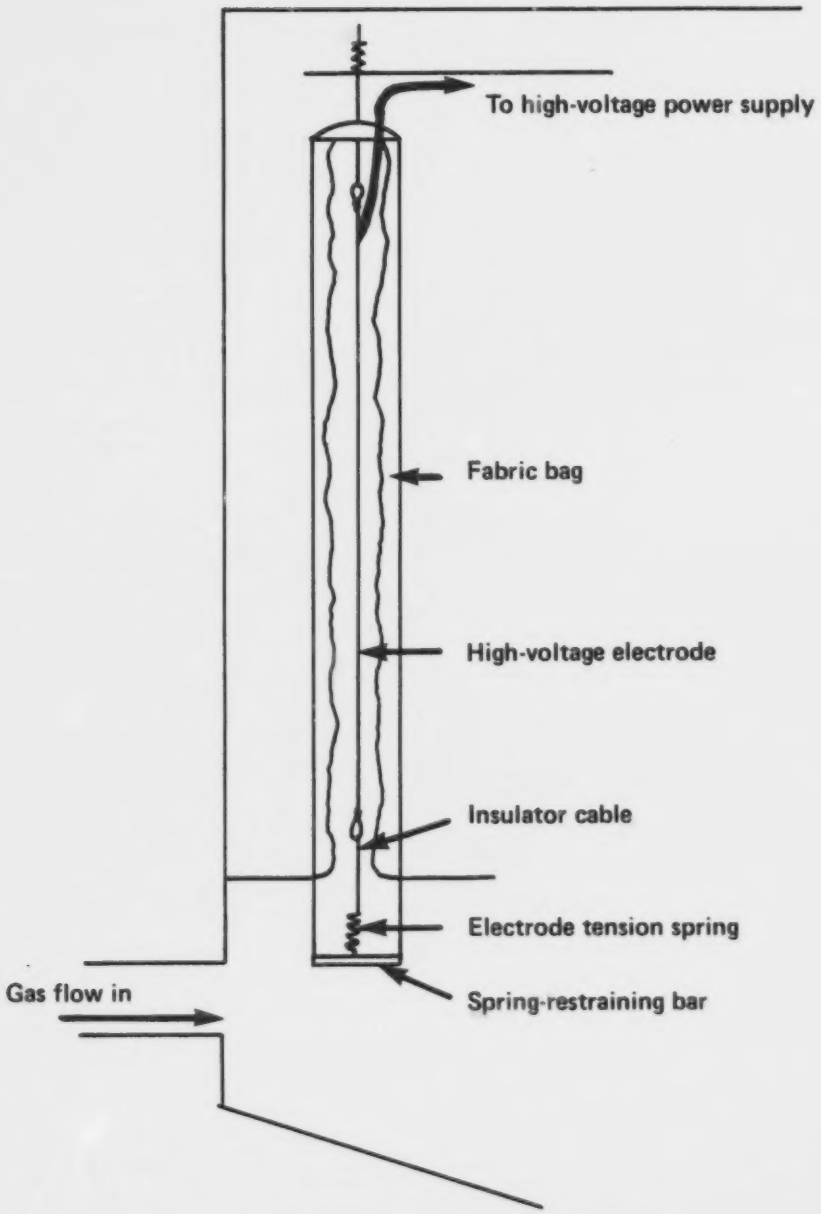

Figure 2. The center-wire configuration of ESFF.

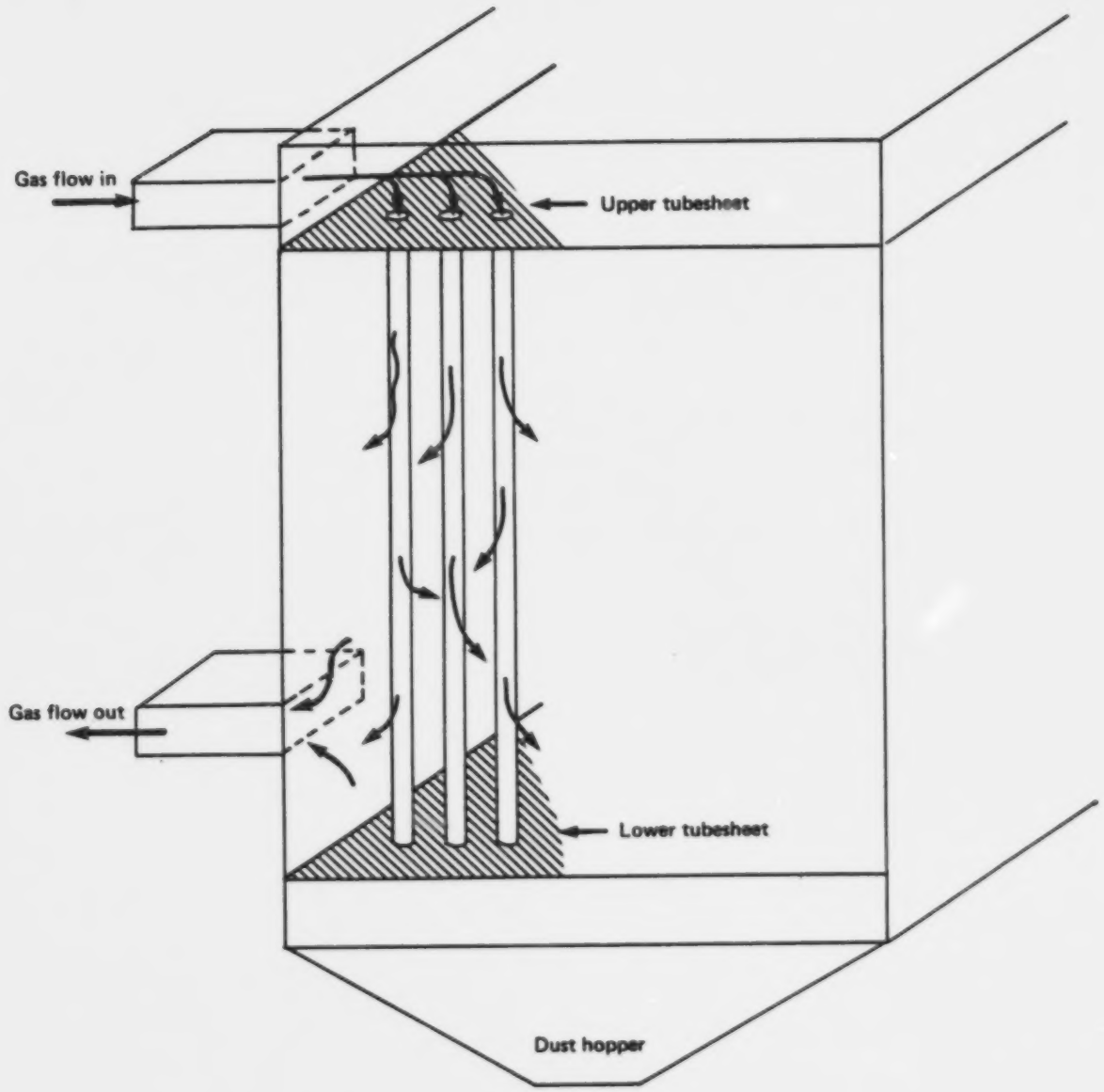

Figure 3. A conceptual design of a top-inlet baghouse.

This report will describe the results of a large-scale pilot plant evaluation of these new technologies. The sections that follow contain detailed information on the pilot plant hardware, including some novel features of the monitoring of baghouse performance. In addition, the study results and an analysis of the economic feasibility of the advanced ESFF technology will be presented.

SECTION 2

PILOT PLANT DESIGN

A fabric filter pilot plant was designed to filter coal fly ash from a slipstream off of two spreader stoker-fired boilers. The plant was located at Cherry Point Marine Corps Air Station (CPMCAS) in Havelock, North Carolina. The boilers are rated at a maximum of 77,500 pounds of steam per hour. Only one boiler was on line at any given time during the pilot plant test. The fuel for the boilers was an eastern coal with 1 percent sulfur, 5 percent water, and a heat content of 31,600 kJ/kg (13,600 Btu/lb). The ash from the boiler had a high unburned carbon content. As a result, its electrical conductivity was relatively high for a coal ash.

The pilot plant is shown schematically in Figure 4. Identical baghouse compartments were located side by side, next to a test trailer. Each compartment was fed by a separate fan with a capacity of 19.82 m^3/min (700 ft^3/min) air drawn from a common duct. This common duct draws gas from the inlet of the electrostatic precipitators downstream of each boiler. The inlet ducts could be closed off in the event that one of the boilers was taken off line. A single reverse-air fan provided ambient air for cleaning each compartment. Dust removed from the bags during cleaning was deposited in large barrels located beneath each compartment hopper. These ash barrels were emptied three times a week by plant personnel.

From the outset, the focus of this project was to demonstrate the feasibility of advanced ESFF rather than to try to optimize design and/or operation considerations. As a result, the only tests performed were those that were required to demonstrate the ESFF "effect" and, to a small degree, define the operating range of advanced ESFF. Also, site considerations required that all of the testing be performed within a 12-month period (from February 1985 to February 1986). This requirement affected the experimental design. The central problem was in making arrangements to test three types of filtration strategies--advanced ESFF, top-inlet, and

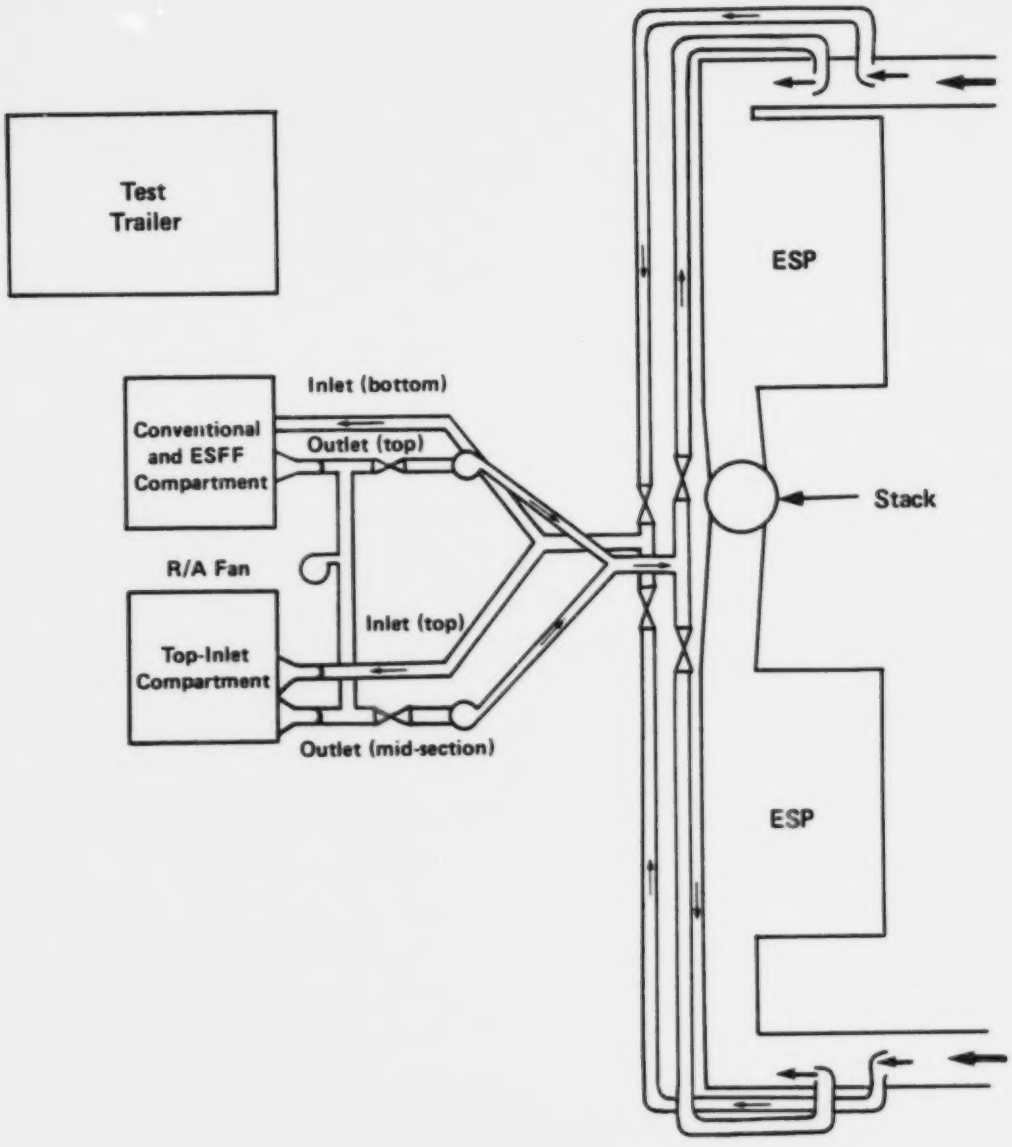

Figure 4. Schematic of Cherry Point pilot plant.

conventional bottom inlet (as a control group)--in two compartments while maximizing the amount of run-time for each condition. One possibility would have been to establish one compartment of conventional bags as the control group and the other compartment as the test group, first with ESFF and later with top-inlet bags. This design would have limited the amount of testing time for each strategy. Instead, a set of individual bag-flow monitors (IBFMtm) was used, permitting simultaneous operation of advanced ESFF and conventional bags in a single compartment. This left the other compartment free to operate with the top-inlet design.

An IBFM™ consists of a calibrated orifice plate placed at the inlet of the bag on top of the compartment tubesheet. Pressure taps located on the upstream and downstream side of each orifice plate provide a mechanism for measuring the orifice pressure drop. Data on the pressure drop, temperature of the gas, and calibration allow the flow into each of the bottom-inlet bags (conventional and ESFF) to be calculated. This information, along with the tubesheet pressure drop and inlet dust concentration, can then be used to calculate the dust cake's specific resistance and residual drag. The comparison of these parameters yields a figure of merit for evaluation of the ESFF design. A similar comparison was possible with the data from the top-inlet compartment. The greatest advantage of testing the ESFF and conventional bags in a single compartment is that the different bags were exposed to identical conditions, providing increased confidence in the comparison of the results for the two bags. Some effort was required to eliminate flow and temperature differences between the top-inlet and bottom-inlet compartments.

The ESFF electrode system is illustrated in Figure 5. A hook was attached to the bottom of a conventional bag cap. An insulating cable, consisting of a bundle of three Teflon® cables 0.3175 cm in diameter (1/8 inch), was suspended from this hook in the bag cap. The lower end of the insulating cable was connected to the high-voltage electrode, which was a twisted stainless steel cable 6.4-m long (21 ft). A spring was attached to the bottom of the electrode cable, and the bottom of the spring was attached to a second bundle of three Teflon® cables. This lower cable was held securely in the center of the bag tube by a restraining bar at the inlet to the bag thimble. The purpose of the spring was to provide

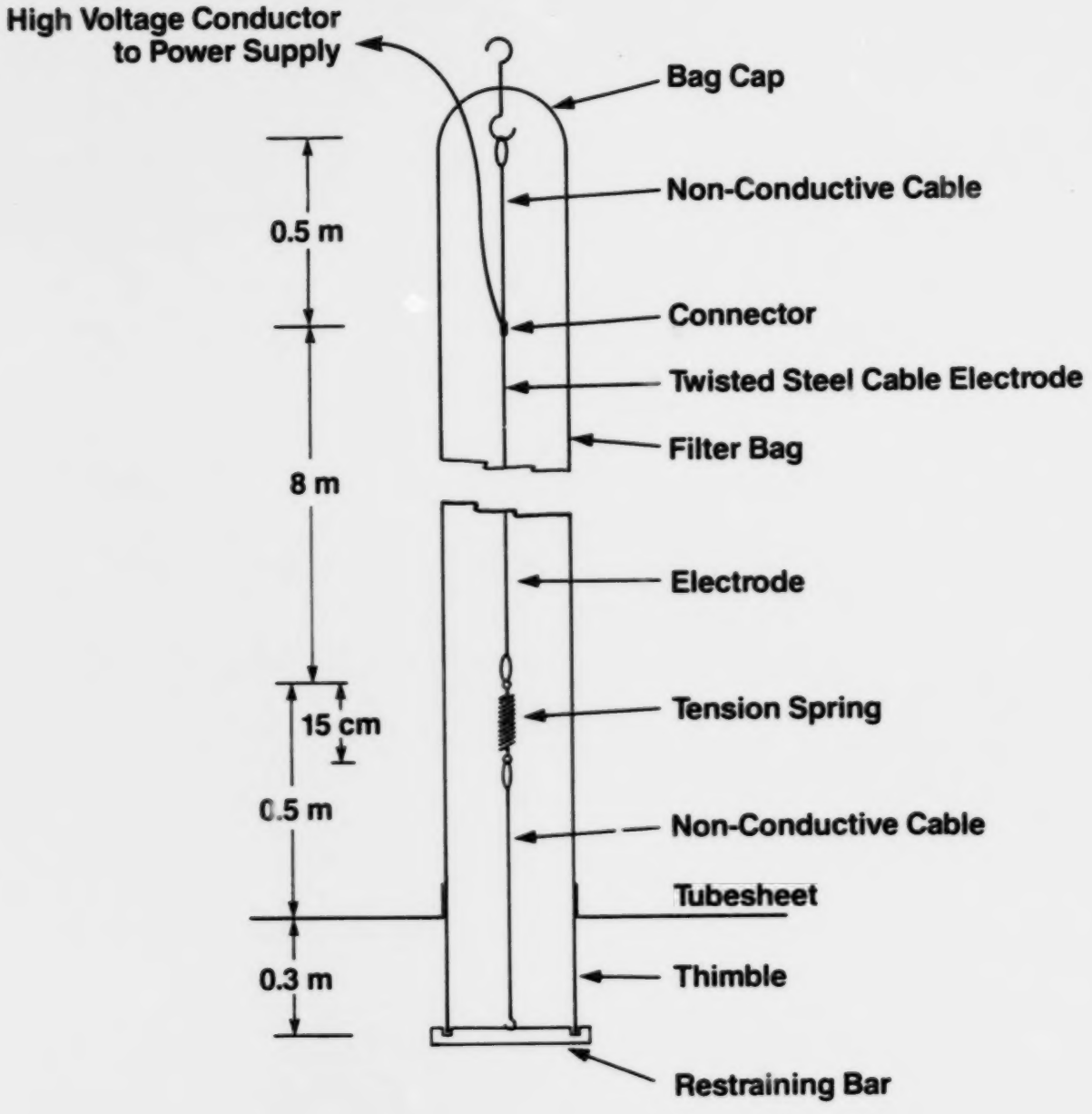

Figure 5. A prototype electrode design for implementation of advanced ESFF.

flexibility in the electrode while the bag was being tensioned. The voltage to the electrode was supplied by a high-voltage wire sheathed in Teflon® tubing that passed through a hole drilled in the bag cap. All of the bags in the bottom-inlet baghouse were fitted with these center wire electrodes, but they were divided into two sets that were wired in parallel. Only one set of bags was electrified at any time. The schematic for the voltage control on the electrodes appears in Figure 6. A variable transformer controlled the output from a 60-kV power supply. The high-voltage output was scaled down to a range of 0 to 6 volts for input to the data logging equipment. The current to ground was also measured at the power supply.

All of the bags used in this study were woven from J. P. Stevens 648 fabric. When the study began it was not known how well the dust/fabric combination would serve as a ground plane for the electric field. There was a question as to whether the dust/fabric combination would be conductive enough to provide a ground plane. To test the importance of this conductivity, two of the bags in the bottom-inlet compartment (one control and one ESFF) were made from fabric that had small diameter, stainless steel electrodes woven into it at regular intervals. All of these fabric electrodes were connected to the grounded compartment structure.

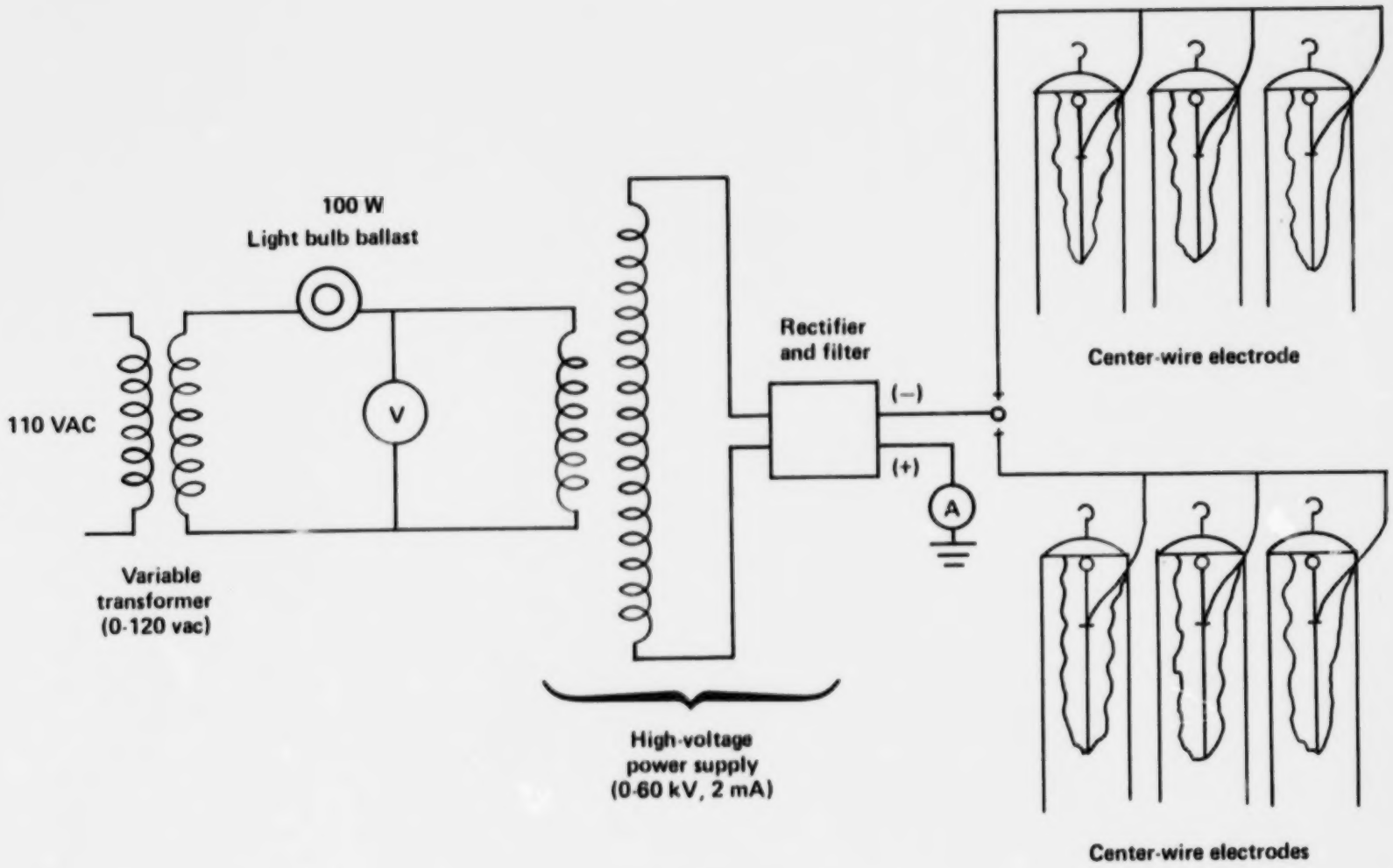

Figure 6. Power supply control circuit.

SECTION 3

DATA ACQUISITION AND ANALYSIS

DATA ACQUISITION SYSTEM

As previously mentioned, site considerations required that all testing be completed within 1 year and cost considerations weighed heavily against keeping an operator on site every day. Given these two restraints, the logical course of action was to automate the data collection and retrieval. A system was designed for the automatic measuring, recording, and computer storing of pressures, temperatures, and electrical conditions. Off-the-shelf computer hardware and software permitted the long-distance retrieval of recorded data. This system offered many advantages, the most important being the elimination of labor costs for data collection and computer entry (along with potential transcription errors) and long-distance data retrieval. The latter permitted daily data analysis and monitoring of pilot plant operation.

The measurements required for this system included the temperatures, tubesheet and orifice pressure drops, electrical conditions, and dust-inlet loadings. All measurements were automated except the dust-inlet loadings, which were measured during two site visits according to standard EPA Method 5 procedures. For the automated measurements, the temperatures were measured with Type K thermocouples fitted with electronic icepoints. Tubesheet pressure drops and orifice pressure drops for compartment inlet and outlet flows were measured with pressure transducers rated 0 to 2.5 kPa (0 to 10 inches H_2O). The IBFM pressure drops were measured with smaller transducers (-1.25 to 1.25 kPa [-5 to + 5 in. H_2O]). Voltage output from the electrode power supply was stepped down from 0 to 60 kV to 0 to 6 V, and electrode current to ground was measured directly. All of these signals were fed into a Molytek Model 2702 Programmable Datalogger, which served as the interface to a Tandy 1200 microcomputer. At 10-minute intervals, the datalogger transmitted instantaneous readings to the computer. Custom-developed software controlled the reading and storage of data from the datalogger. The Concurrent PC-DOS operating system permitted

the simultaneous execution of the data collection/storage program and remote communications. A high-speed modem with an automatic answering feature, in conjunction with the multiuser capability of the DOS, permitted home-office engineers to call the onsite computer and read data files from previous days. Once retrieved, the data were read into a worksheet developed with the Lotus 1-2-3 (C) program for graphing and analysis.

DATA ANALYSIS

The only disadvantage of using two different types of filtration in a single compartment is that it precludes the possibility of making an "on-the-spot" evaluation of performance based on tubesheet pressure drop. That is, the data must be analyzed before the results are known. This disadvantage is far outweighed by the advantages of the experiment, as outlined in Section 2.

Data analysis begins with the commonly accepted model of pressure drop behavior in fabric filters; it is assumed that the drag across the filter increases linearly with increasing dust load:

$$\Delta P = V(t) \bullet S(t) = V(t) \bullet (S_e + K_2 \bullet W(t-t_{clean})) \qquad (1)$$

where

ΔP is the pressure loss across the dust on the filter

$V(t)$ is the filtration velocity at time t

$S(t)$ is the drag across the filter at time t

S_e is the effective residual drag

K_2 is the specific resistance of the dust

$W(t-t_{clean})$ is the mass of dust deposited per filter area since the most recent bag cleaning at time t_{clean}.

The areal dust load is a function of the rate at which dust is deposited on the filter:

$$W(t-t_{clean}) = C_i \bullet \int_{t_{clean}}^{t} V(\tau)\, d\tau \qquad (2)$$

where

C_i is the dust concentration at the inlet of the filter

$V(\tau)$ is the filtration velocity at time τ.

The pressure drop (ΔP) was recorded at 10-minute intervals throughout the filtration cycle. Likewise, the flow orifice pressure drop at the inlet to both the top- and bottom-inlet compartments were recorded. From these pressure drops, the flow rates into the compartments were calculated. Because there were two types of bags in the bottom-inlet compartment, the individual bag flows were measured via flow orifices. The individual bag face velocities were then computed from the inlet flow rates and the known filtration area of the bags. Face velocity for the top-inlet compartment was computed as the ratio of the compartment inlet flow to the total bag area because it was assumed that all bags in the top-inlet baghouse performed identically. Once the filtration velocities were known as a function of time, the dust load $W(t-t_{clean})$ was calculated from the measured filtration velocity $V(t)$ and the inlet dust concentration C_i. Bag drags (S) were computed as the ratio of tubesheet pressure drop to flow velocity.

From these calculated values, the residual drag S_e and the specific resistance K_2 in Equation 1 were determined by linear regression of drag against dust load. In this manner, the values of K_2 and S_e were calculated for each of the bags and for the top-inlet compartment. These constants were then used to compare the performances of the different filtration techniques. The lower the K_2 value, the lower the rate of pressure rise. Similarly, the smaller the value of the residual drag S_e, the lower the overall pressure drop will be. These values were then used to extrapolate the behavior of the new filtration techniques to other conditions. Of course, the reliability of such extrapolations declines as the proposed conditions depart from the conditions under which the values were measured.

Of the parameters listed in Equations 1 and 2, the one known with the least certainty is the inlet dust concentration, C_i. In the bottom-inlet compartment, it can be shown that the ratio of K_2 values is independent of this inlet dust concentration if that concentration remains relatively

constant throughout the filtration cycle. This also holds true for the ratio of the residual drags. The comparison of K_2 values between the bottom-inlet and top-inlet compartments is more susceptible to errors due to differences in inlet dust load and variations of dust load throughout the cycle. To address this problem, plant personnel weighed and emptied the ash barrels regularly and kept records of the barrel weights. These weights, combined with the measured flow since the barrel was last emptied, provided an independent check of inlet concentrations.

SECTION 4

RESULTS

The pilot plant was installed during February and March of 1985 and was brought on line in April. The hardware was debugged during April and May of that year, and data collection began in early June. The plant ran continuously from June until the end of September, except for brief periods during which: the boiler was down (coal elevator repair); the boiler was switched from Number 1 to Number 2 (requiring a manual switching of some pilot plant valves); and an electrical outage caused the fans to switch off automatically and required a manual restart. At all other times, the plant ran with a minimum of operator intervention and collected data automatically.

BOTTOM-INLET COMPARTMENT

The feasibility of advanced ESFF and (to a lesser extent) top-inlet filtration depends upon the ability to operate at higher face velocities than a conventional bag. Therefore, the focus of testing these new filtration technologies was to determine if they could operate for prolonged periods with face velocities that were substantially higher than a conventional filter. Given this goal, and considering the limited amount of time available for operation, a test plan was drawn up specifying one long test. Rather than conducting a variety of short experiments to test the importance of many parameters, the plan called for a single experiment in which the filtration velocity was gradually increased. This made it possible to determine the limits on the operating range for the ESFF and top-inlet bags. This experiment was especially important because it was impossible to explicitly set the flow rate through the conventional and ESFF bags; that is, it was only possible to set the overall flow rate to the bottom-inlet compartment. The distribution of flow between the ESFF and conventional bags was determined by the drag differential between the two sets of bags.

The results of this experiment are shown in Figure 7. The figure shows the cycle-average air-to-cloth ratio for each bag in the bottom-inlet compartment versus the cycle number. The cycle number refers to a 12-hour filtration/cleaning cycle (i.e., 11 hours, 50 minutes filtration and 10 minutes cleaning). Thus, each point in the figure represents a half-day average of air-to-cloth ratio for a given bag. Cycle Number 1 roughly corresponds to mid-June when the data acquisition system was debugged and brought on line. Cycle Number 150 occurred in late September. There is no exact correspondence between calender days and cycle numbers because the pilot plant did not operate on some days; hence, no cycle numbers correspond to that day.

With the exception of the data from cycle Number 50 to cycle Number 70, the curves are separated into two "families." The upper set of curves corresponds to the advanced ESFF bags, and the lower set of curves corresponds to the conventional filter bags. The overall air-to-cloth ratio (compartment inlet flow/total compartment bag area) increases from an initial value of 0.55 m/min (1.8 ft/min) to 0.79 m/min (2.6 ft/min) at cycle Number 50. Shortly after this flow change was made the reverse air fan failed. This caused the erratic data shown in Figure 7. During a site visit to repair the fan, two of the bags in the bottom-inlet compartment (one electrified and one conventional) were removed to increase the air-to-cloth ratio to 0.91 m/min (3.0 ft/min). Another operating modification was made at cycle Number 137 to increase the air-to-cloth ratio to 1.26 m/min (4.15 ft/min). The tubesheet pressure drop ranged from a low of 0.1 kPa (0.4 inches H_2O) at an air-to-cloth ratio of 0.55 m/min to a high of 0.87 kPa (3.5 inches H_2O) at an air-to-cloth ratio of 1.26 m/min. This information is not directly useful except as an indication that pressure drop did not hinder the operation at higher flow rates.

The results in Figure 7 are a convenient summary of data for the entire test program. A more meaningful comparison requires an analysis such as that described in Section 3. The bag-flow data for a given cycle must be analyzed in conjunction with the pressure drop data and the dust inlet concentration. The bag flows and pressure drops were measured automatically, but the dust concentration was measured manually. The dust

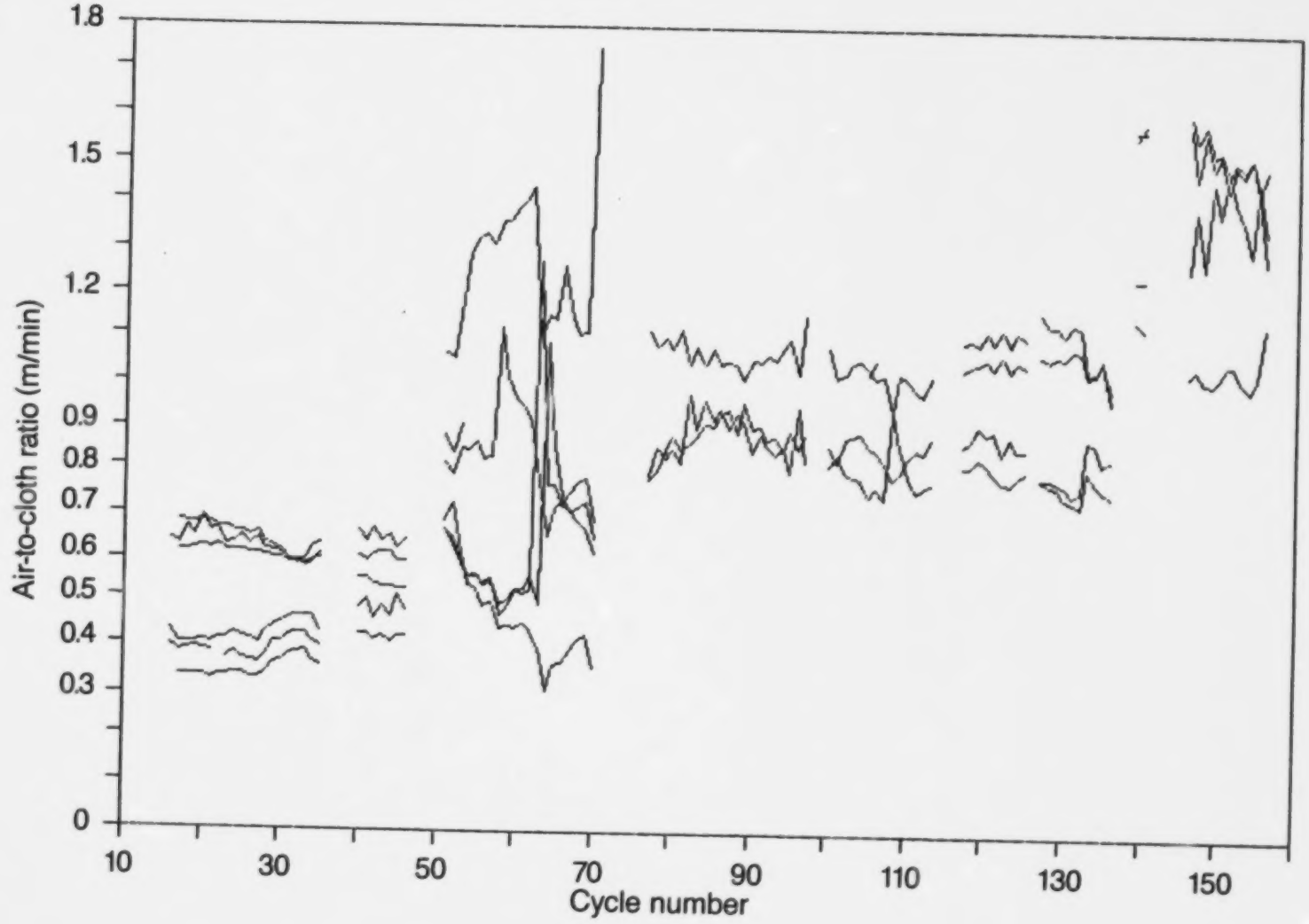

Figure 7. Average air-to-cloth ratio for each bag in bottom-inlet compartments.

concentration was measured during two site visits, according to standard EPA Method 5 procedures. The results of these measurements summarized in Table 1, with the particle penetration data, show a significant difference between the top-inlet and bottom-inlet concentrations. Also, the concentrations changed significantly between the first measurement in April and the second measurement in July. The particle penetrations listed in the table seem high but they are not unreasonable for new bags (less than 3 months old). In a routine operation, penetration through an advanced ESFF baghouse probably would be the same as that of a conventional baghouse.

Each data point in Figure 7 represents the average of a 12-hour cycle. A detailed look at some of the raw data in Figure 7 is presented in Figure 8. The curves (Figure 8) show the IBFM orifice pressure drops for cycle Numbers 126 through 130. Each cycle spans 720 minutes (12 h). At the beginning of each cycle, the orifice pressure drops are relatively close together, indicating a newly cleaned state. As time progresses, the pressure drops diverge, representing a divergence of the flow rates. The upper set of traces represents the advanced ESFF bags while the lower set corresponds to the conventional bags. At the end of the filtration cycle, the flow is stopped, and the bags are cleaned. The presence of the reverse-air cleaning is clearly evident in the negative pressure drops, because the flow of air through the orifice plate at the inlet of the bag is reversed, temporarily reversing the high-pressure/low-pressure orientation of the pressure transducer. The reverse air flow produces this negative pressure spike. The data in this figure can be converted to flow rates with a knowledge of the orifice coefficients. The resulting flows for one set of curves in Figure 8 appear in Figure 9. Specifically, the curves on the far right of Figure 8 were used in the calculations. As expected, the flow curves follow a pattern similar to that of the orifice pressure drop curves.

The parameters K_2 and S_e can be computed from the inlet dust concentration, the individual bag flows, and the tubesheet pressure drop. In Figure 10, the tubesheet pressure drops that correspond to the cycles in Figure 8 are shown. In this figure, the upper curve traces the top-inlet

TABLE 1. PARTICULATE LOADING DATA

Date	4/25/85		7/31/85	
	Loading (gr/scf)	Penetration	Loading	Penetration
Top inlet				
In:	0.1163		0.1868	
Out:	0.0074	6.4%	0.0056	3.0%
Bottom inlet				
In:	0.1622		0.1914	
Out:	0.0081	5.0%	0.004	2.1%

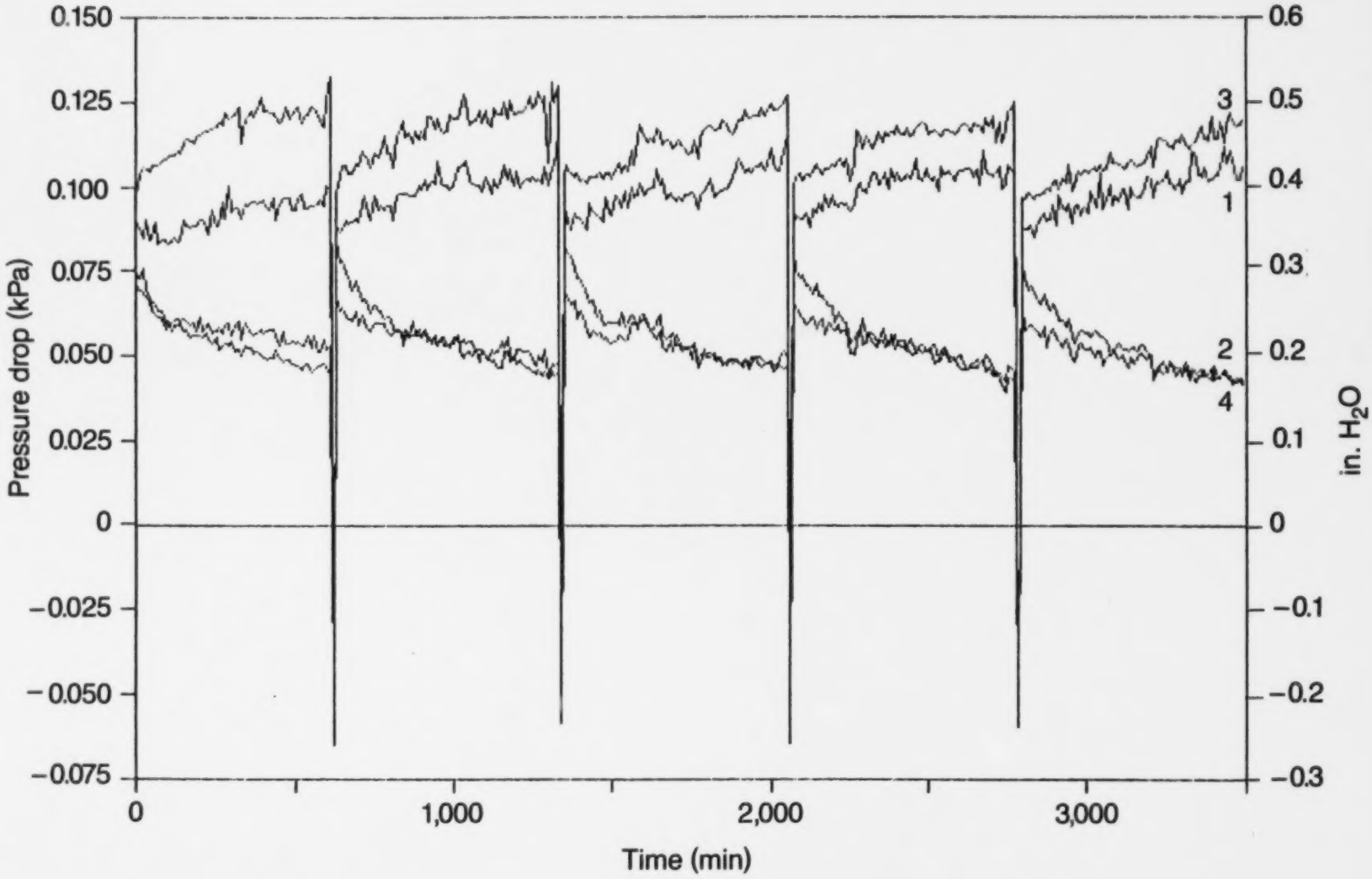

Figure 8. IBFM pressure dropcurves: August 29 through August 31 (numbers 126-130).

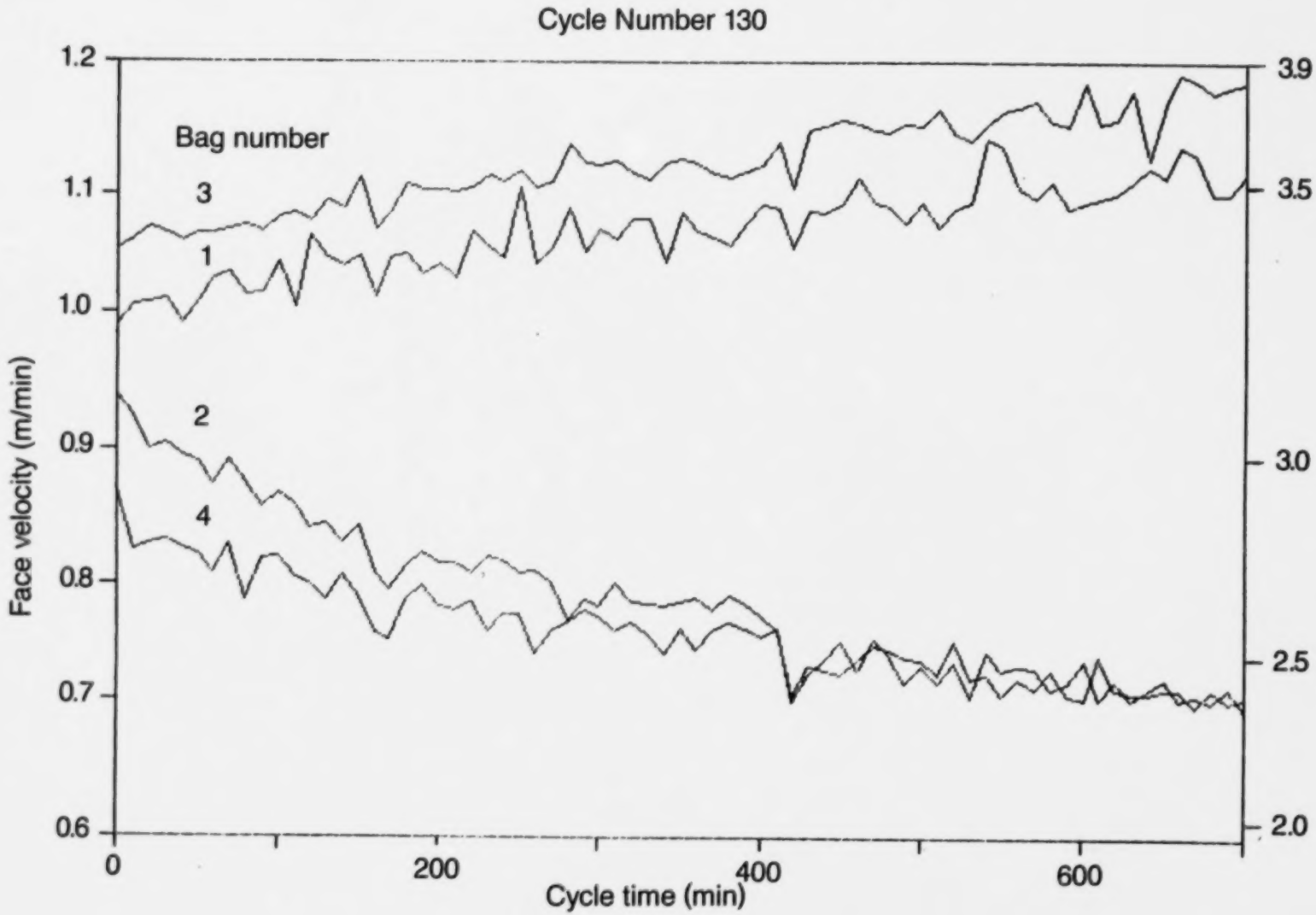

Figure 9. Individual bag-flow data from ESFF pilot plant.

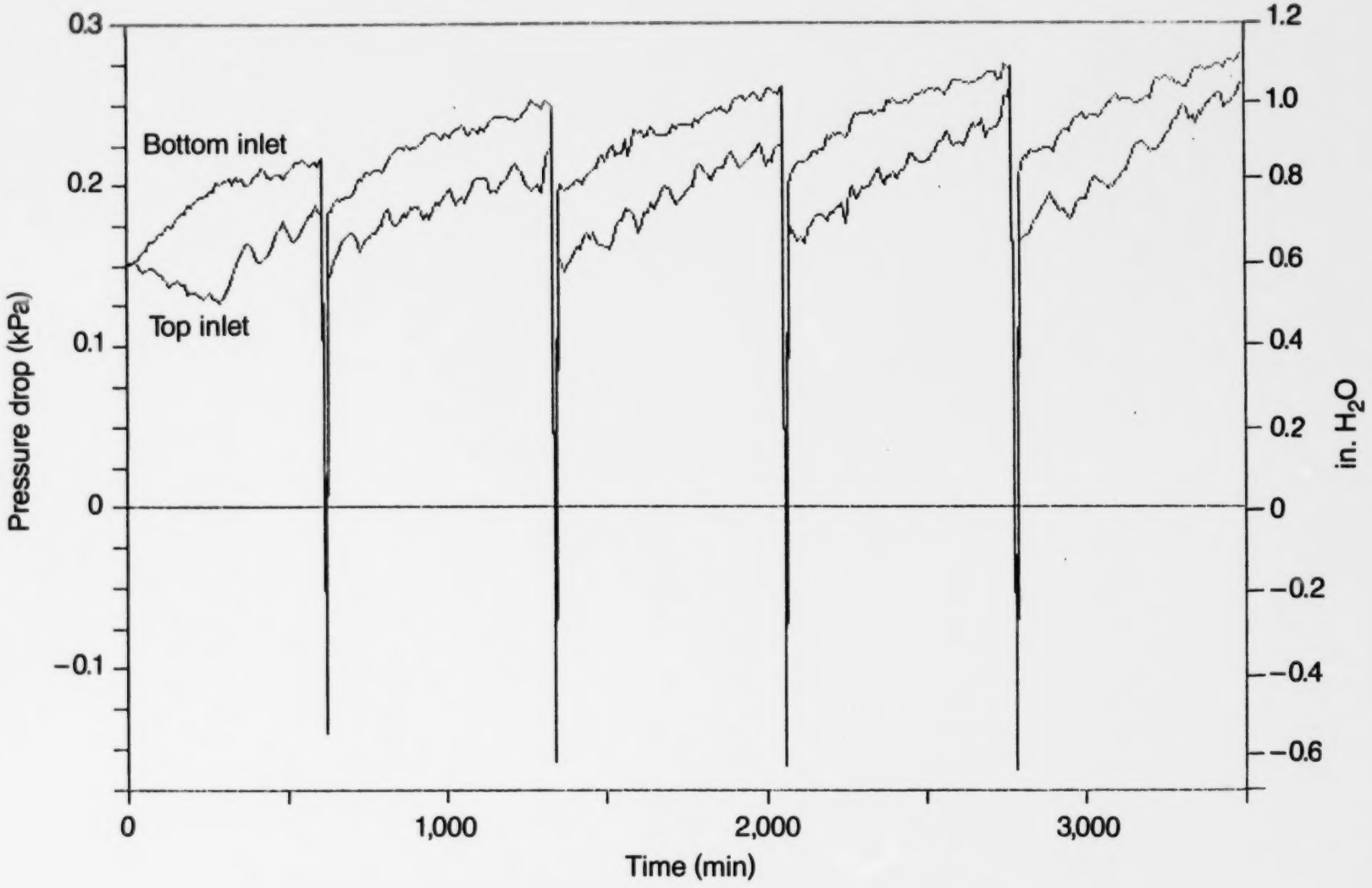

Figure 10. Tubesheet pressure drop for top-inlet and bottom-inlet compartments: August 29 through August 31.

compartment, and the lower curve traces the bottom-inlet compartment. The diagram makes clearly evident the negative pressure spikes caused by the reverse-air cleaning.

From the data in Figure 9 and the dust concentration data, Equation 2 can be used to compute the variation of dust load (kg/m^2) on each bag as a function of time. The ratio of pressure drop to bag flow velocity yields the bag drag. A plot of bag drag as a function of dust load is shown in Figures 11 and 12. The ESFF data appear in Figure 11, the conventional data in Figure 12. The straight line in each figure represents the regression fit to the data. There are two important features to note in these figures. First, the straight lines provide a good fit to the data, indicating that the assumption of a linear relationship between drag and dust load inherent in the data analysis is reasonable. Second, the slopes (i.e., K_2 values) of the two lines are quite different; that is, the drag for an ESFF bag rises much more slowly than that of a conventional bag. Of lesser importance is the fact that the intercept of the two lines is slightly different, the conventional bag having a slightly higher residual drag than the ESFF bag. The important point to be made here is that, by assuming an appropriate model of pressure-drop behavior and measuring the individual bag flows, the values of K_2 and S_e can be determined fairly easily.

This analysis was performed on all of the data collected from the pilot plant. An important practical result of this analysis was the summarizing of large volumes of data (for each bag, during every cycle) into two numbers that can be used for comparison: K_2 and S_e. The complete results of conventional and ESFF K_2 values are summarized in Figure 13. Several features of these results became evident. At the beginning of the test (cycle Numbers 10 through 34), there are two families of curves. The upper set of curves (Bags 1, 3, and 5) corresponds to the K_2 values for the non-electrified bags. The lower set of curves (Bags 2, 4, and 6) shows the K_2 values for the electrified bags. The large gap between them indicates the effectiveness of the center wire electrode at producing more permeable dust cakes. To test the system, the power to the electrified bags was shut off near the end of cycle Number 28. Immediately, the K_2 values of the even-

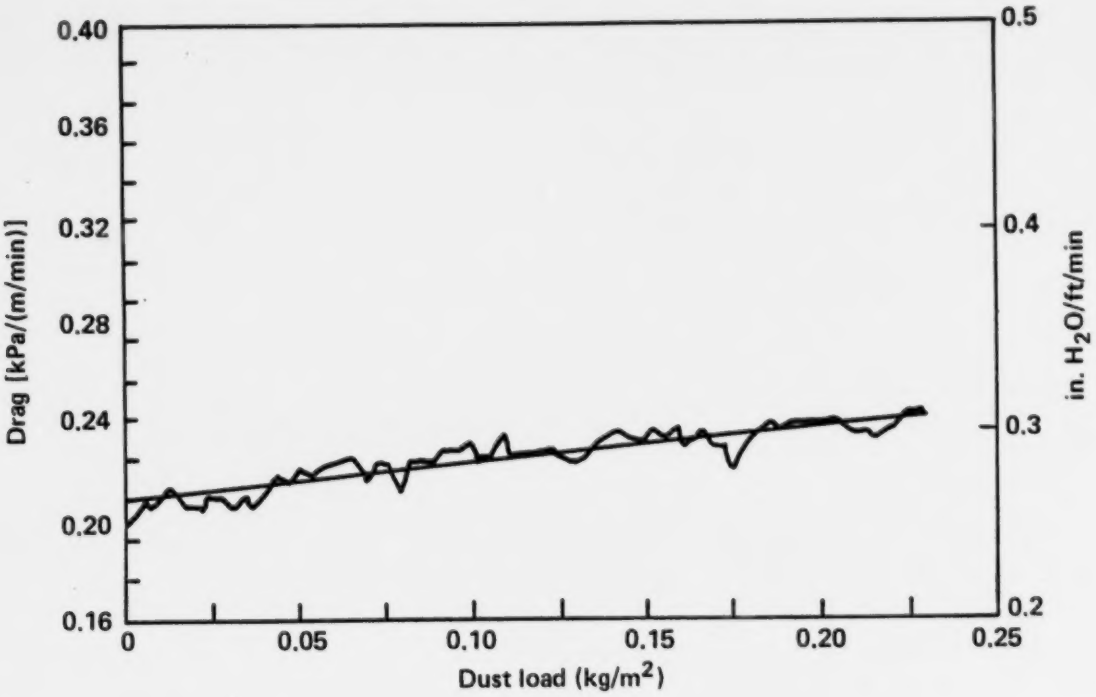

Figure 11. Drag correlation for bag number 1 (ESFF).

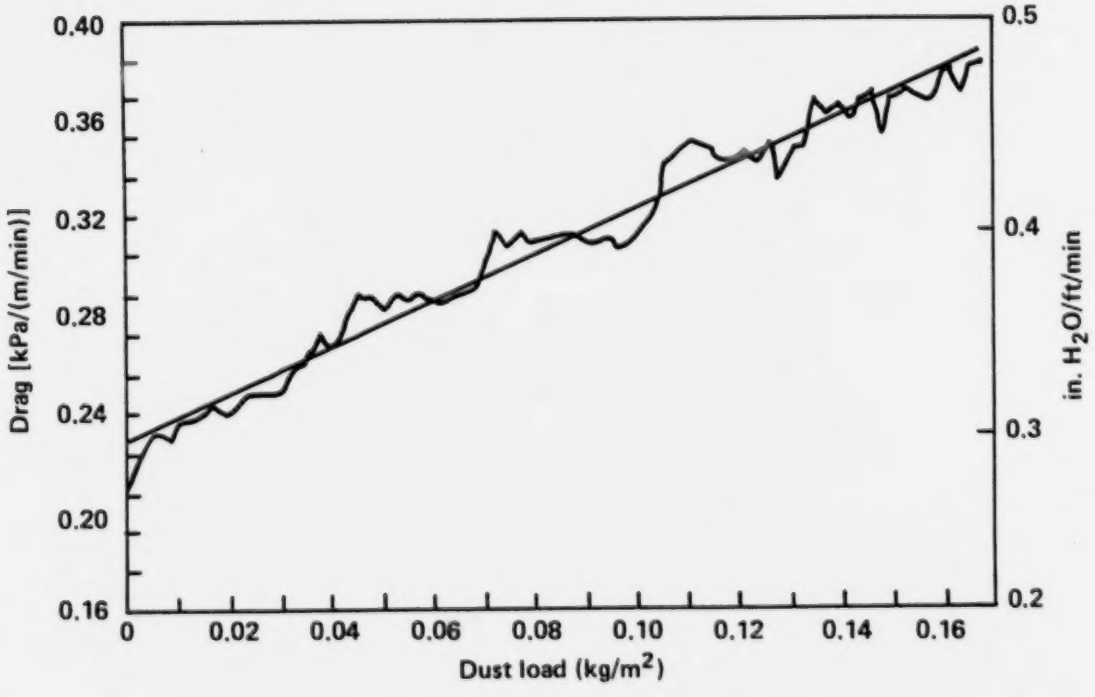

Figure 12. Drag correlation for bag number 2 (conventional).

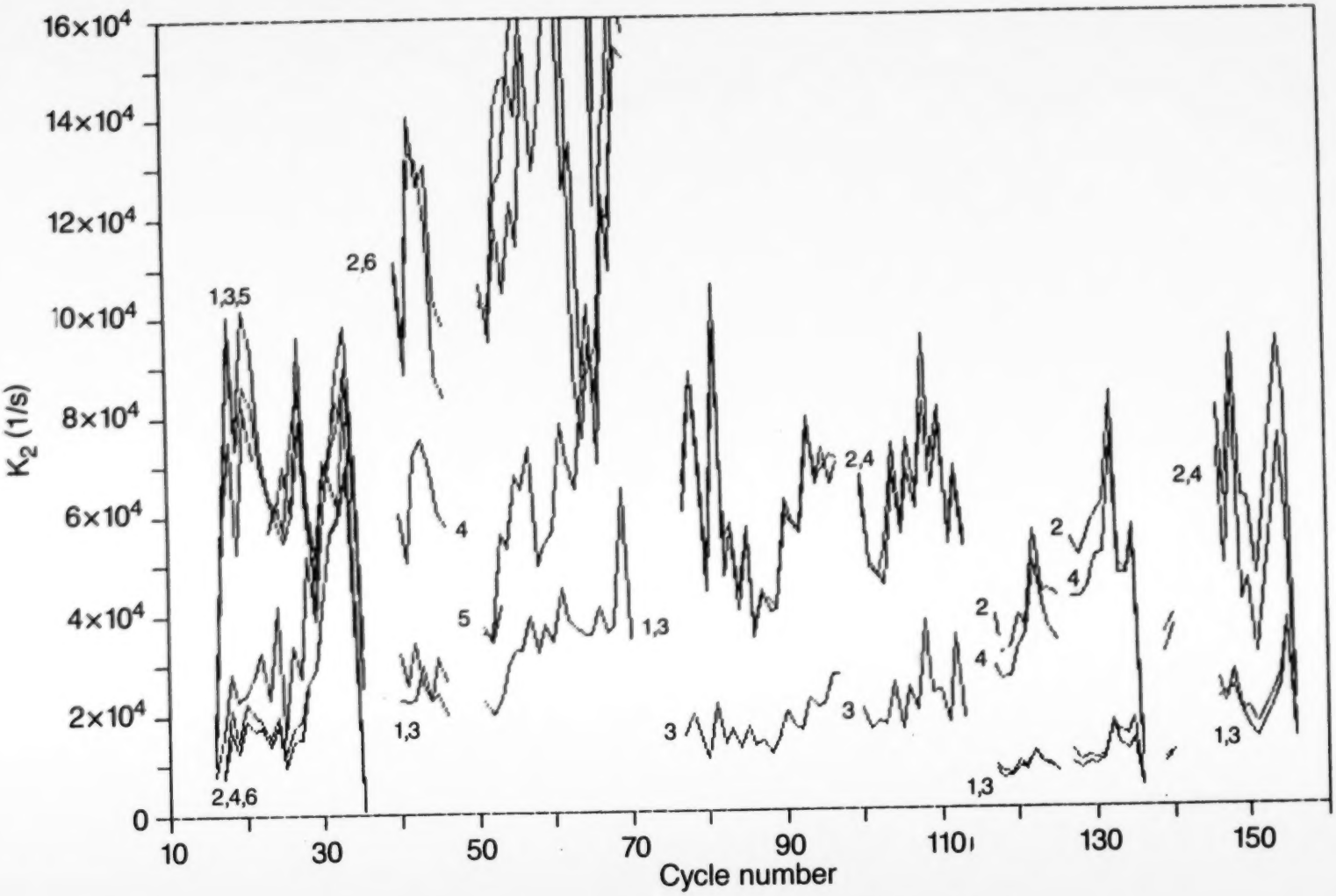

Figure 13. Summary of the specific resistance for each bag in the bottom-inlet compartment.

numbered bags began to rise to the level of the odd-numbered bags. This test demonstrated that the electric field caused the difference in the K_2 values.

Another demonstration of the ESFF effect was performed by turning the electrode power back on, this time with Bags 1, 3, and 5 electrified instead of Bags 2, 4, and 6. The result is seen in Figure 13, between cycle Numbers 40 and 50. The high values of K_2, formerly associated with the odd-numbered bags, are now characteristic of the even-numbered bags. The K_2 values of the odd-numbered bags are now much lower. These results are corroborated by the bag-flow data shown in Figure 14, where the air-to-cloth ratios cross over after the power is switched from the even to the odd bags. As described earlier, the failure of the cleaning fan renders the data from cycle Numbers 50 to 70 virtually meaningless. However, a clear pattern emerges again in Figure 13 after cycle Number 70. The odd-numbered bags (Bags 1 and 3) show a consistent pattern of lower K_2 values than the even-numbered bags (Bags 2 and 4). This difference persisted through the end of the test program.

An interesting feature of the data is the close agreement between bags of a given type. The curves for Bags 2 and 4 are almost indistinguishable, especially between cycle Numbers 70 and 110. No results are shown for Bag 1 during those cycles because of a problem with the IBFM data for that bag. Specifically, ash buildup in one of the pressure taps of the orifice plate caused step changes in the pressure reading for that orifice. However, these step changes clearly did not reflect an actual change of flow. This problem was corrected by altering the procedure for purging the pressure lines.

Determining the specific resistance (K_2) is useful because it allows one to make a comparison of filtration techniques that is independent of filtration velocity, dust concentration, and a number of other parameters. The K_2 results can be further condensed by comparing the average of the electrified bags with the average value of the conventional bags. Figure 15 shows the ratio of K_2, electrified to K_2, conventional. For example, a value of 1.0 means that the rate of pressure rise for an ESFF bag is the same as the rate for a conventional bag, and a ratio of 0.5 means that the

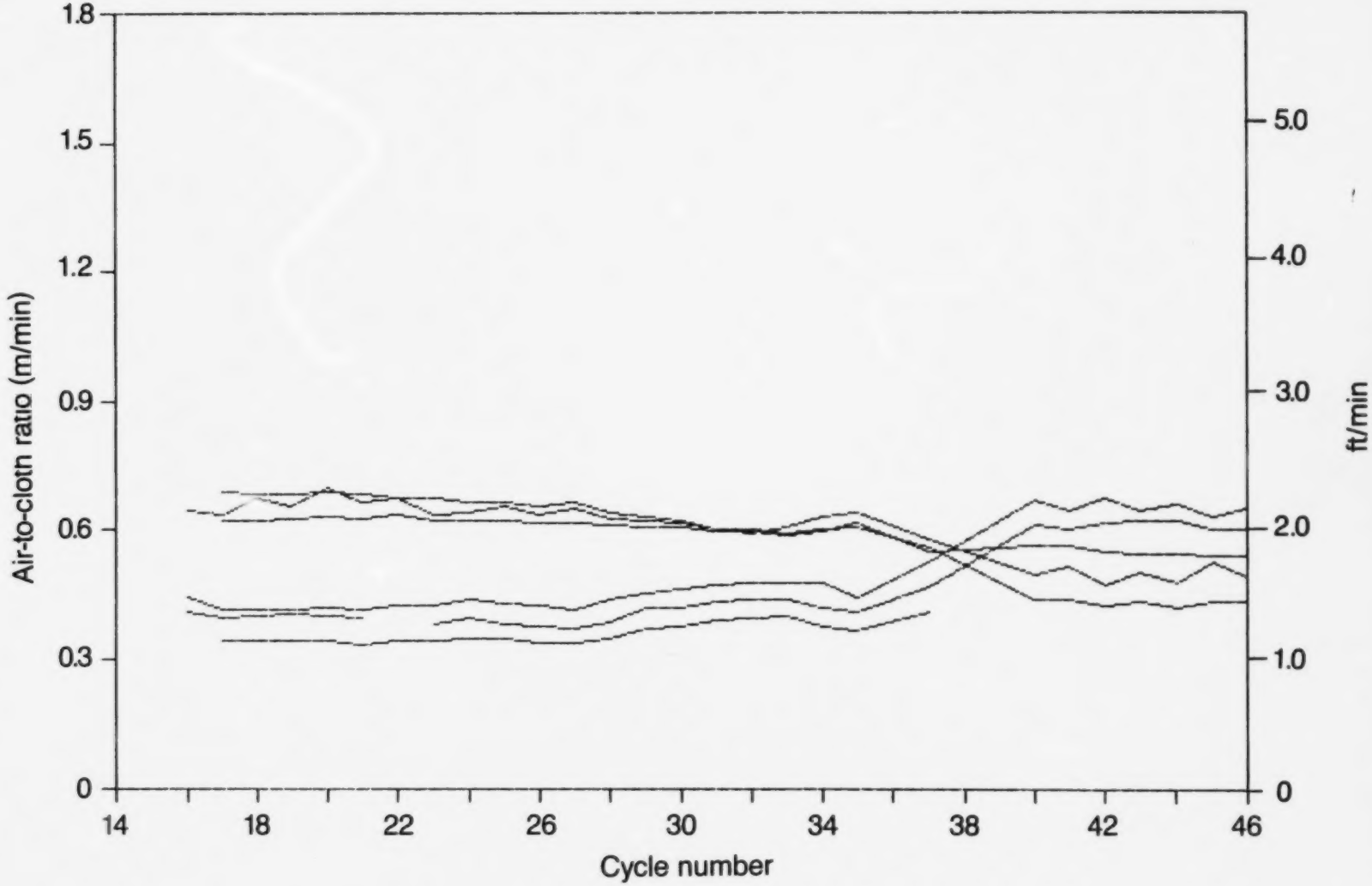

Figure 14. Individual bag-flow data (cycle average air-to-cloth ratio) when the voltage was switched.

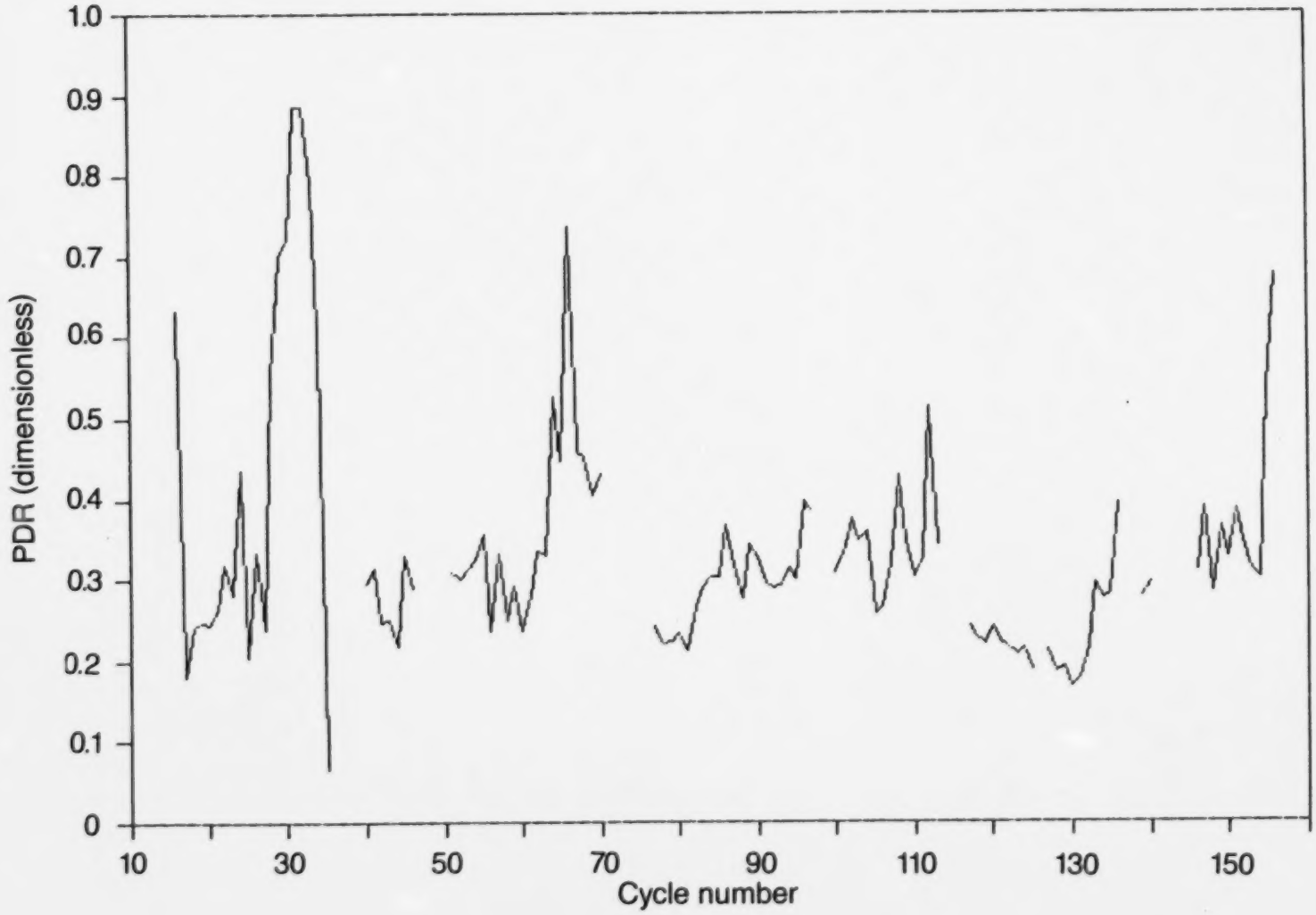

Figure 15. The pressure-drop ratio of specific resistances.

rate of pressure rise for an ESFF bag is half that of a conventional bag. This ratio is identical to the pressure-drop ratio (PDR) used by Miller et al. (2) because it is assumed that drag increases linearly with increasing dust load. The PDR results mirror the operating data from the plant. For example, when the voltage to the ESFF bags was shut off during cycle Number 28, the K_2 value for the ESFF bags began to approach the value of the conventional bags. Thus, the K_2 ratio increased towards 1.0. When the voltage was turned on for the odd-numbered bags, the ratio dropped again. The large peak shown in Figure 15 between cycle Numbers 60 and 70 reflects the erratic data caused by the failed cleaning fan during those cycles.

With the exception of these excursions, the ratio tends to fluctuate around a mean of roughly 0.3. If this experiment had been conducted with two identical compartments (one of which used conventional technology and the other ESFF technology), the average pressure drop across the ESFF compartment would be 70 percent less than the average pressure drop across the conventional compartment.

The other parameter that resulted from the data analysis is the residual drag, S_e, summarized in Figure 16. During the early operation of the pilot plant there was a significant difference between the residual drags of the electrified and nonelectrified bags. This difference began to disappear when the voltage was switched from the even-numbered bags to the odd-numbered bags (cycle Number 28). Once again, the effects of the reverse-air fan failure are evident in the data (from cycle Numbers 50 to 70). After this problem was corrected, a difference between the electrified and nonelectrified bags seemed to develop, though the evidence is weak.

The cycle-average current and voltage of the ESFF electrodes appear in Figures 17 and 18. These quantities were measured at the power supply rather than at each electrode. It is assumed that the parallel circuitry from the power supply to the electrodes ensures the existence of identical conditions at all electrodes. Each point in these figures represents a 12-hour average of the voltage or current values. The voltage data show a fairly stable operation, ranging from approximately 18 kV to 36.7 kV. This is reflected in the detailed cycle data, which also showed little variation

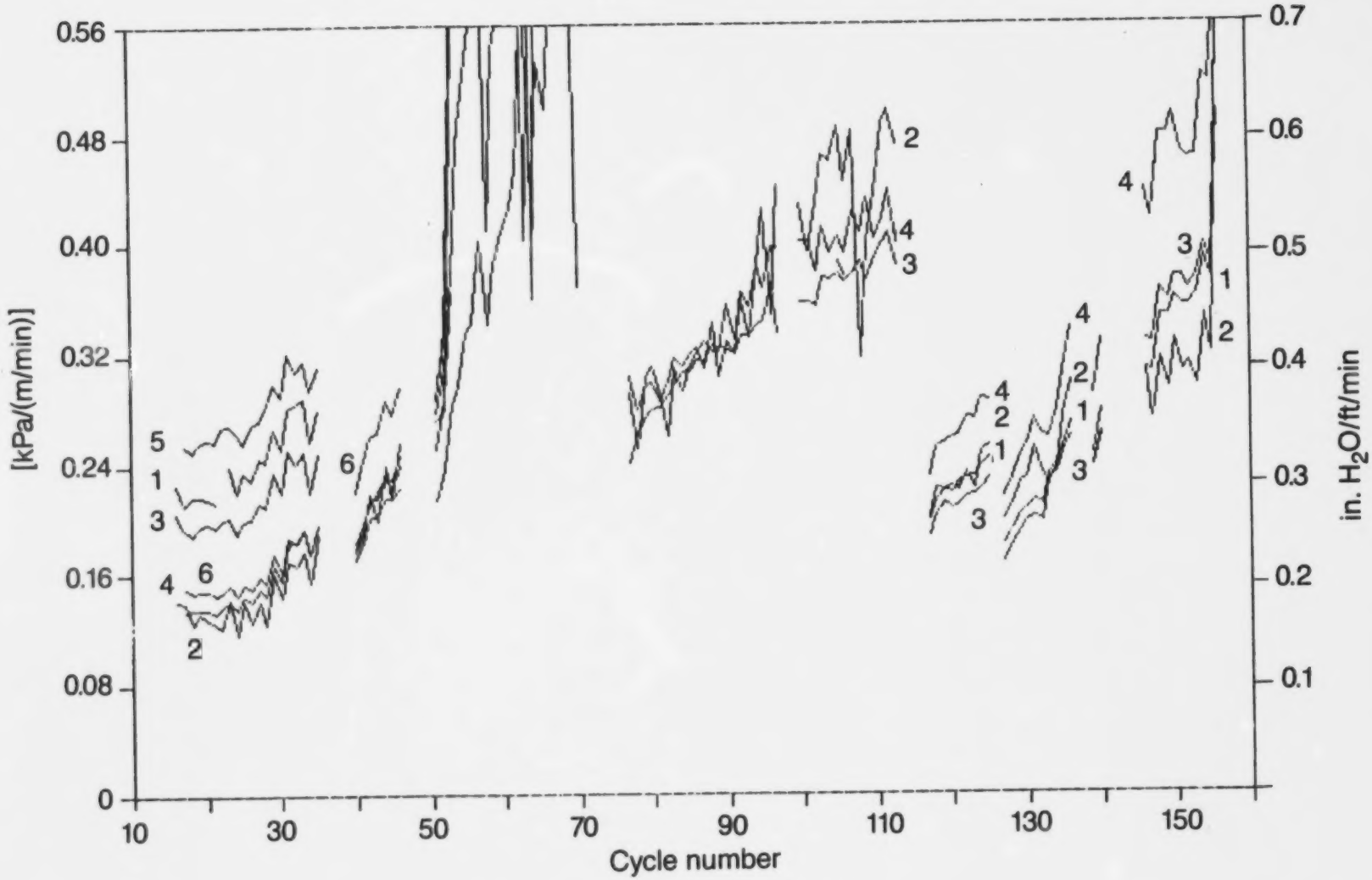

Figure 16. Residual drag results (drag at the beginning of the filtration cycle).

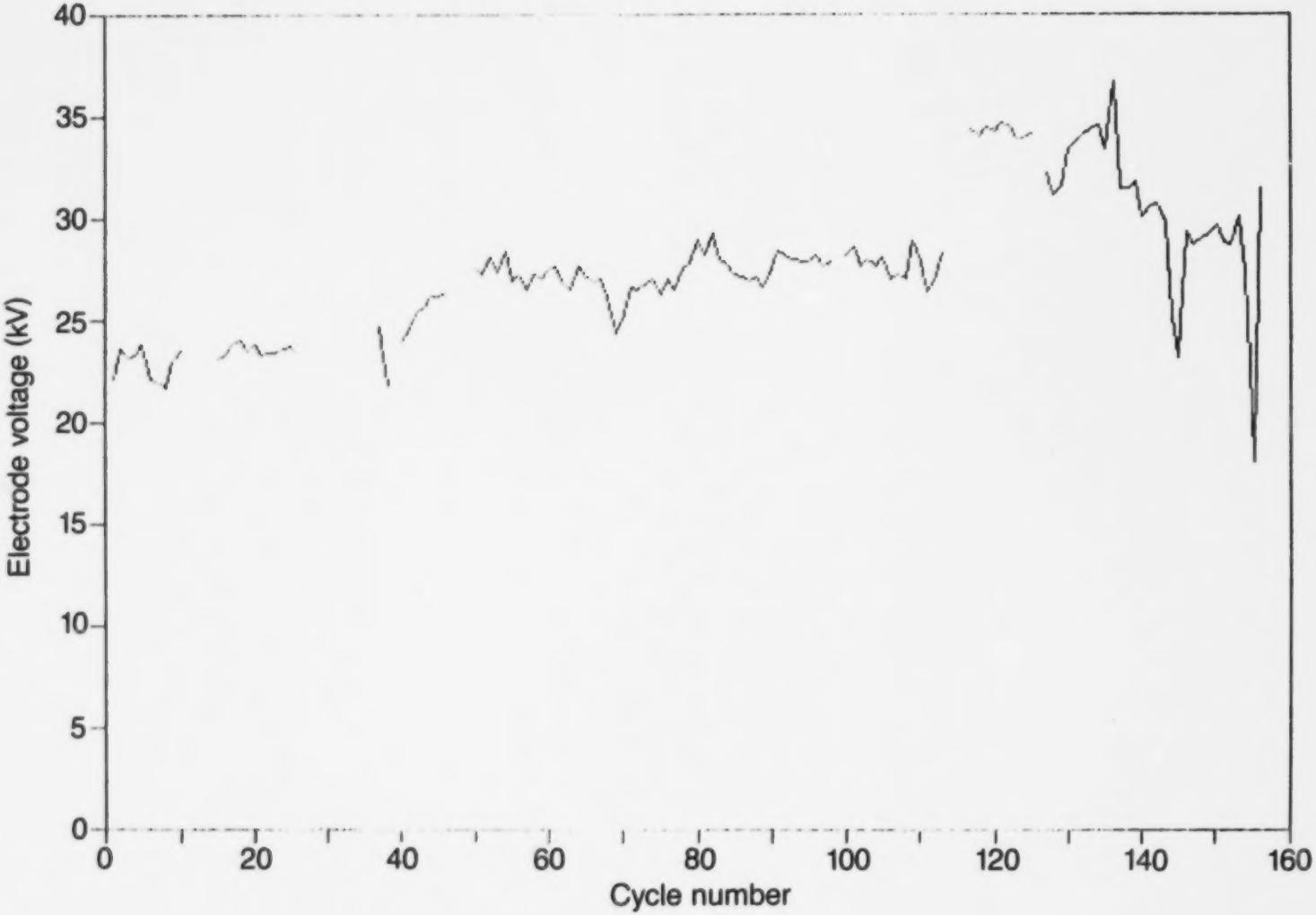

Figure 17. Average electrode voltage for each cycle.

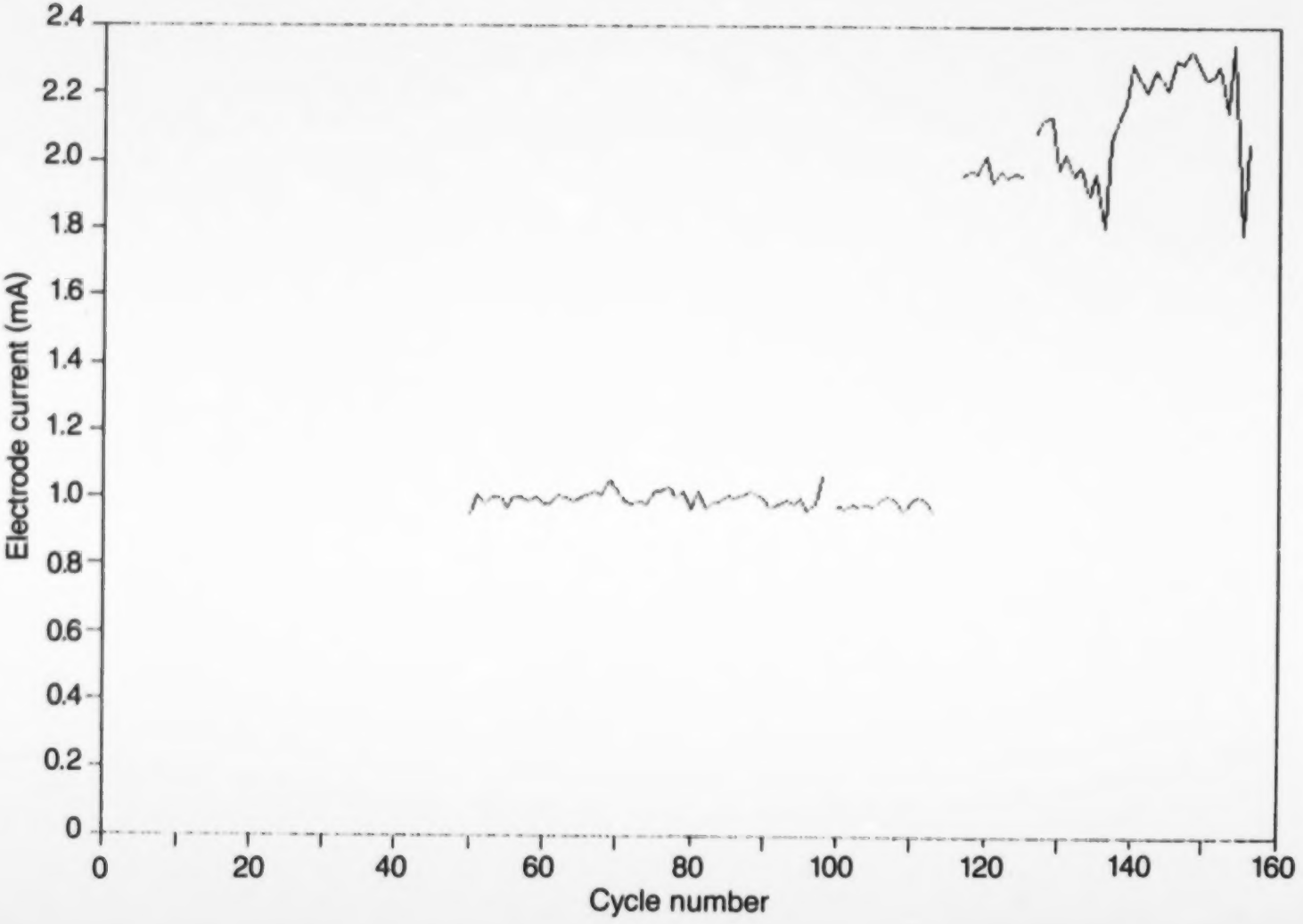

Figure 18. Average current output from the power supply.

of voltage throughout each cycle. Beginning with cycle Number 127, the noise in the data increases markedly. The cause for these wide fluctuations is not known; however, it may be explained in conjunction with the current data (Figure 18). The earliest current data (cycle Numbers 50 to 115) are fairly stable at a value of roughly 1 mA. At the beginning of cycle Number 116, the 100-W ballast light bulb in the power supply control circuit was replaced with a 200-W light bulb. This modification permitted the power supply to operate at full capacity (2 mA) and caused the step change in current from 1 to 2 mA at cycle Number 116. This step change, although less pronounced, also occurs in the voltage data. Shortly after the power was modified, the voltage and current started to exhibit wide fluctuations in the cycle average values.

These fluctuations are possibly due to variations in the conditions within the compartment. Because the power supply is operating at full capacity, there is no reserve to compensate for changes in electrical conditions within the baghouse (caused by temperature, humidity, or other variations). It is interesting to note that during the brief period between cycle Numbers 116 and 127 (when the current was fairly stable at 2 mA and the voltage was stable at 34 kV), the PDR approaches its lowest value (Figure 15).

TOP-INLET COMPARTMENT

The measurements for the top-inlet compartment were much simpler than those for the bottom-inlet compartment because it was assumed that all of the top-inlet compartment bags were identical. That is, it was assumed that there was a single K_2 value that characterized all of the bags in the compartment at a given time. Likewise, the residual drag (S_e) was assumed to be the same for all of the bags. These assumptions eliminated the need for individual bag-flow monitors in the top-inlet compartment because the overall compartment behavior was considered synonymous with individual bag behavior. Therefore, by measuring the compartment inlet flow and the tube-sheet pressure drop, the compartment drag and dust load can be calculated. As before, regression analysis of drag versus dust load on the bag yields the specific resistance (K_2) and residual drag (S_e). These values can then be compared with the average of conventional bag values from the bottom-inlet compartment.

The test plan for the top-inlet compartment was very similar to the plan for the bottom-inlet compartment. The face velocity was increased from an initial level of 0.55 m/min to a maximum of 0.79 m/min. The results from these tests were marred by two problems. The aforementioned breakdown of the cleaning fan (from cycle Numbers 50 through 70) affected the top-inlet house in the same way that the bottom-inlet house was affected. In other words, the bags were not cleaned regularly, if at all. The uncontrolled buildup and removal of dust on the bags make a comparison of the data for this period meaningless.

A second cleaning problem developed with the top-inlet compartment after the reverse-air fan was repaired. A loose wire on a solenoid valve caused one of the flow-control valves to close partially or not at all. The net effect was an absence of cleaning in the top-inlet compartment for cycle Numbers 77 through 113. This problem is illustrated in Figure 19, where the residual drag is plotted against the cycle number. The plant operation was normal for cycle Numbers 10 through 51. However, after the reverse-air fan failed, the residual drag began to climb. The term "residual drag" implies that the bag was cleaned, but this did not occur. Thus, to avoid confusion, one should think of the ordinate in Figure 19 as the drag at the beginning of the filtration period. The figure shows that the top-inlet compartment was affected much more adversely by the first cleaning failure than was the bottom-inlet compartment. Although the reverse air fan was repaired after cycle Number 70, the problem of the loose wire on the solenoid valve began to affect the data. Once again, the drag measured at the beginning of the filtration cycle began to climb. The diagnosis of the problem was difficult because it was intermittent. Sometimes the valve would close partially, causing the flow (and hence, tubesheet pressure drop) to fall, but the reverse air would not have produced any cleaning.

Thus, the information received from the computer over the modem gave conflicting signals as to the status of the compartment. Eventually it became clear from the data that no cleaning was taking place. The problem was diagnosed after a prolonged, onsite observation of the cleaning sequence. After this problem was repaired, the compartment was returned to

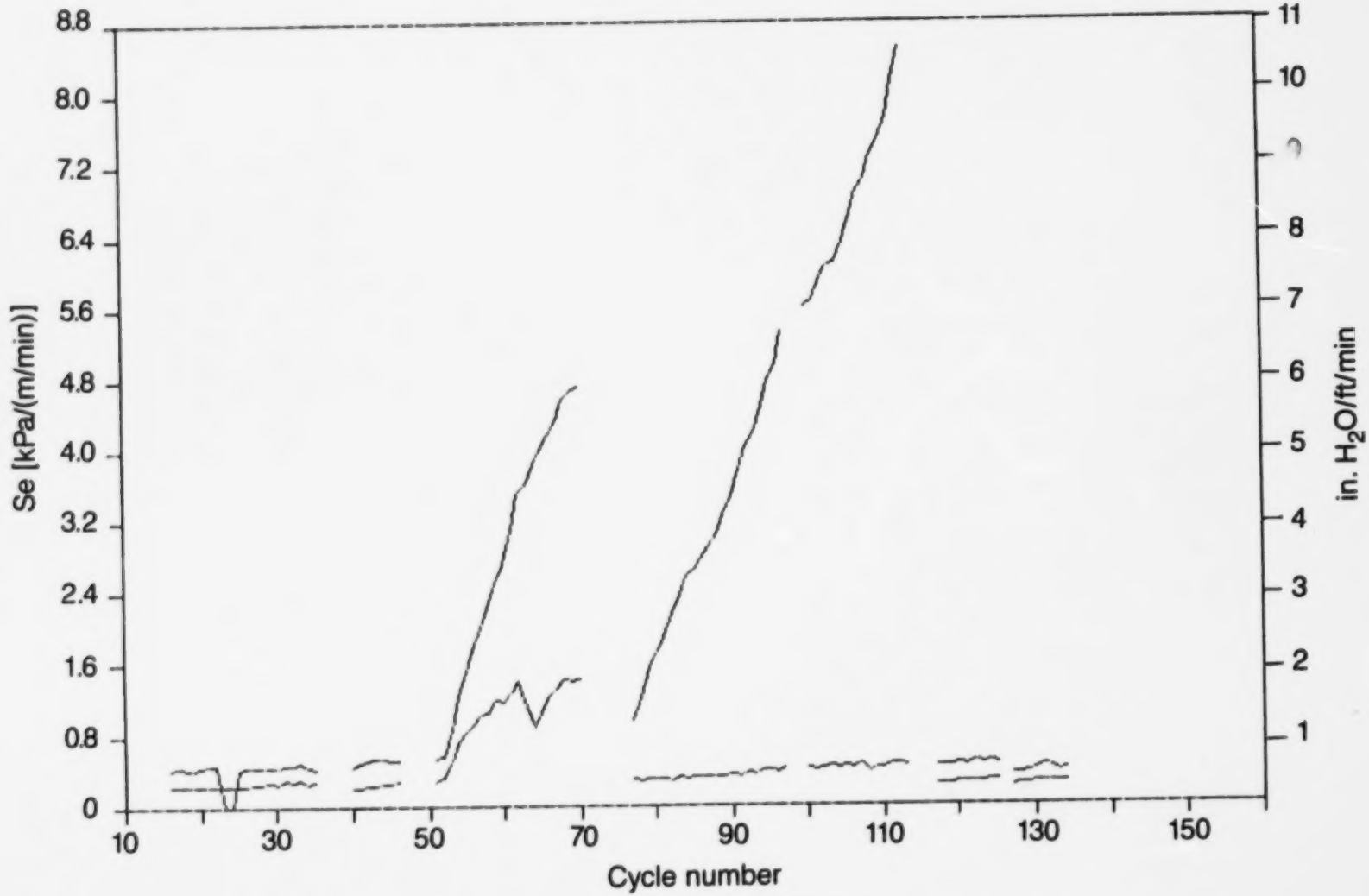

Figure 19. Residual drag for conventional bags (bottom inlet) versus top-inlet bags.

service. The residual drag returned to a level that was characteristic of the early cycles, although it was still greater than the residual drag of the conventional, bottom-inlet bags.

The cleaning problem strongly affected the specific resistance values for the top-inlet compartment. These results are summarized in Figure 20. At the beginning of the test program, the top-inlet K_2 appears to be larger than the bottom-inlet value, but the results are scattered. It is interesting that the top inlet K_2 increased markedly when the air-to-cloth ratio was increased from 0.55 to 0.79 m/min at the start of cycle Number 40. The data for cycle Numbers 50 to 115 are difficult to compare because the top-inlet compartment was not cleaned at regular intervals. After the cleaning problem was repaired (cycle Number 117), the top-inlet baghouse once again showed a higher K_2 value than did the bottom-inlet baghouse. Considering the small amount of data with which reliable comparisons can be made, it is unlikely that sound conclusions can be drawn from the operation of the top-inlet compartment.

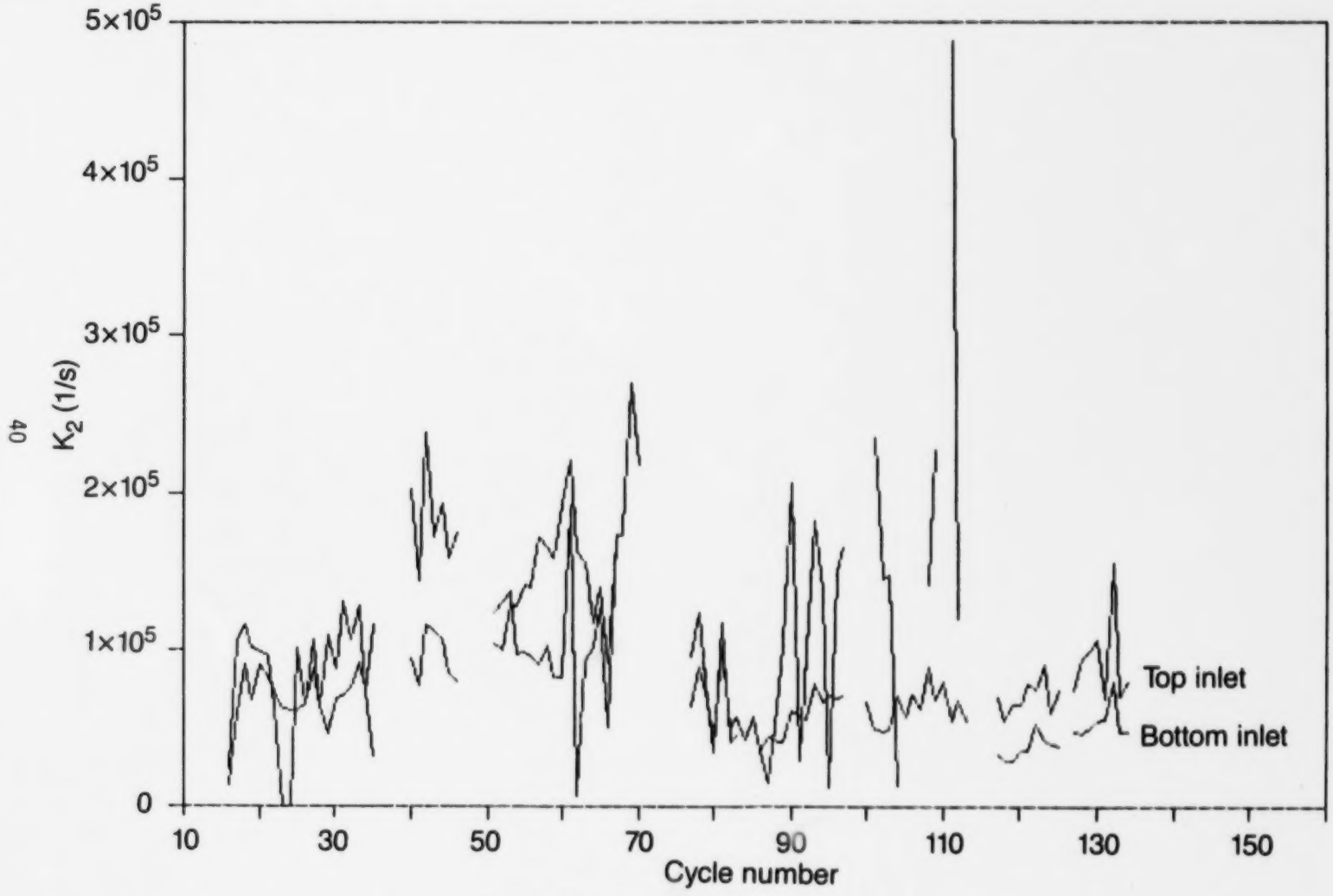

Figure 20. Specific resistances for conventional bags (bottom inlet) versus top-inlet bags.

SECTION 5

ECONOMIC ANALYSIS OF ADVANCED ESFF

The pilot plant results show that advanced ESFF can greatly reduce the rate of pressure rise of a baghouse. This fact can be used to economic advantage. For a fixed average pressure drop, an advanced ESFF baghouse will be smaller than a comparable conventional baghouse. The purpose of this economic analysis is to determine whether the smaller size of an ESFF baghouse offsets the cost of additional hardware.

Typical flange-to-flange hardware costs amount to approximately $172 per square meter of fabric area for baghouses on the scale of 1415 m^3/min (50,000 acfm). An ESFF baghouse would have the additional costs of ESFF electrodes (estimated at $21.50 per square meter of fabric), power supplies ($16.10 per square meter of fabric), and miscellaneous hardware and installation costs ($25,000). Installation costs include a minimum of $160,000 with an additional cost of $103 per square meter of fabric area. Based on these unit cost estimates, the capital cost of a conventional baghouse with an air-to-cloth ratio of 0.61 m/min was compared with the capital costs of three different sizes of ESFF baghouses (0.61, 0.91, and 1.22 m/min). The results of these calculations are shown in Table 2. The expected cost savings are plotted in Figure 21 as a function of air-to-cloth ratio.

Operation and maintenance costs were also considered in the economic analysis. A conventional baghouse with an air-to-cloth ratio of 0.61 m/min was compared with ESFF baghouses of 0.61, 0.91, and 1.22 m/min. The major components of the operation and maintenance costs for this size of baghouse are the bag replacement cost, equipment maintenance cost, and fan electricity cost. (The cost of electricity to run the ESFF electrodes was small compared with these major factors.) The bag replacement cost was based on an assumed bag cost of $10.76 per square meter ($1/ft^2$). Two cases were considered based on bag lives of 2 and 4 years. Equipment

TABLE 2. ADVANCED BAGHOUSE CAPITAL COST COMPARISON

	Conventional	ESFF		
	G/C = 0.61	G/C = 0.61	G/C = 0.91	G/C = 1.22
Flange to flange	$400,000	512,500	350,000	268,750
Installation	400,000	400,000	378,373	323,750
Total installed cost	800,000	912,500	728,333	592,500
Percent savings	0	-14%	+ 9%	+26%

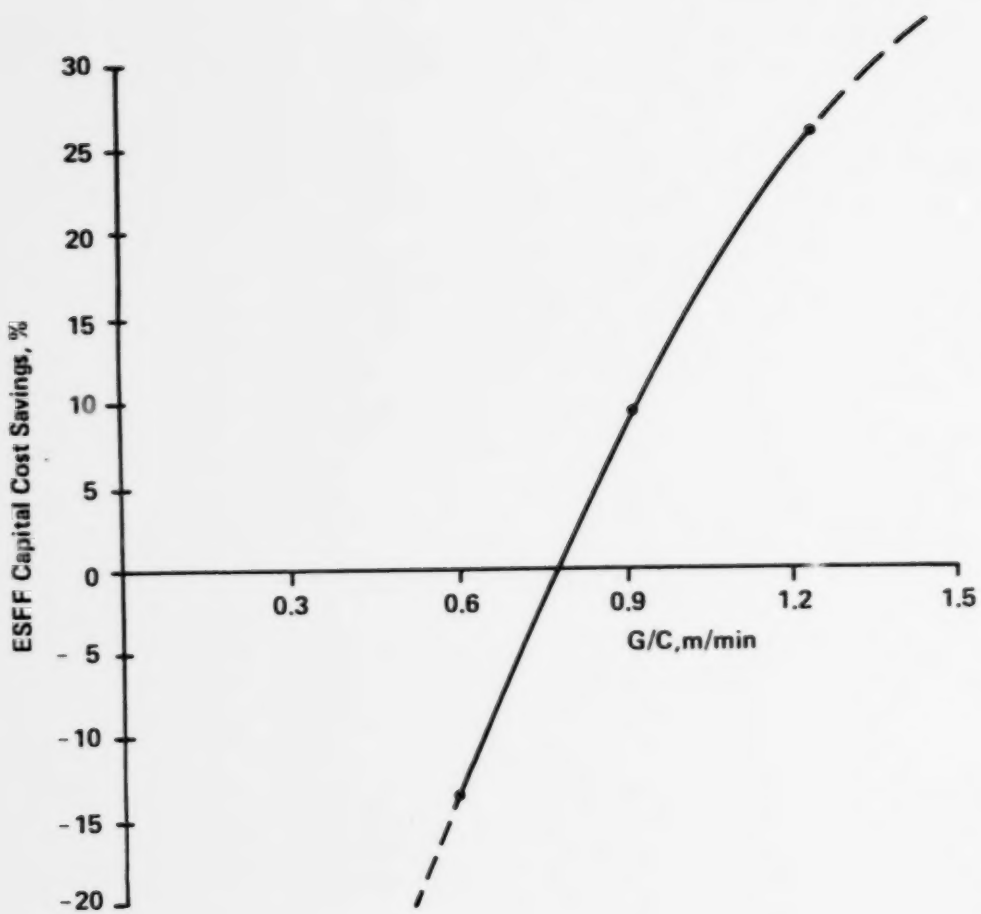

Figure 21. ESFF capital cost savings.

maintenance costs were assumed to total 3 percent of capital costs and the fan electricity cost is proportional to the product of gas flow and pressure drop. The gas flow for this study was constant.

As described earlier, the pressure drop depends on the residual drag (S_e) and specific resistance of the dust cake (K_2). The results in Section 4 indicate that an ESFF baghouse can be expected to have a specific resistance equal to 30 percent of that of the conventional baghouse. This value was used to estimate the pressure drop. Two values were considered for the residual drag. In Case I, the residual drag for the ESFF baghouse was the same as the conventional baghouse. In Case II, the residual drag of the ESFF baghouse was assumed to be half of that of the conventional baghouse. Although there is little evidence to support this assumption based on the results of the current study, laboratory and pilot plant studies of other ESFF geometries have shown a large difference in residual drag.

Based on these assumptions of air-to-cloth ratio, bag life, specific resistance, and residual drag, the annual operating and maintenance costs were computed (Table 3). The annual savings, computed as the percent difference between the ESFF and conventional costs, are plotted in Figure 22.

TABLE 3. ANNUAL OPERATING COST COMPARISON

Case	Bag life	Conventional	ESFF G/C = 2	ESFF G/C = 3	ESFF G/C = 4
I	2	$42,875	$41,875	$37,542	$38,188
	4	36,125	35,125	33,042	34,813
II	2	$42,875	$37,188	$30,510	$28,813
	4	36,125	30,438	26,010	25,438
		Percent annual operating cost savings			
I	2	0	2	12	11
	4	0	3	9	4
II	2	0	13	29	33
	4	0	16	28	30

Case I; PDR = .3, $(Se)_{ESFF} = (Se)_{Conv.}$

Case II; PDR = .3, $(Se)_{ESFF} = .5\ (Se)_{Conv.}$

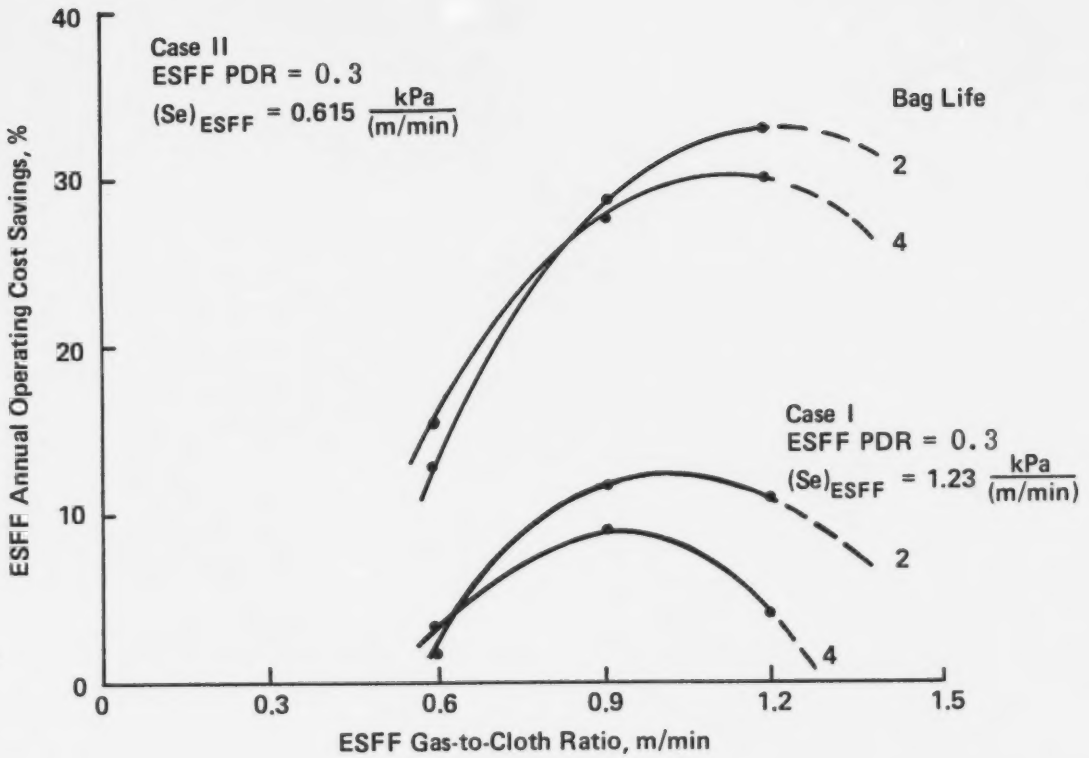

Figure 22. Annual ESFF operating and maintenance cost savings.

SECTION 6

DISCUSSION

HARDWARE

The results of the preceding section show that advanced ESFF is a promising technology. An important aspect of the technical feasibility of a project is the reliability of the hardware. A new technology must be able to operate for long periods of time without operator intervention. Fortunately, this pilot program has shown that the initial design of the advanced ESFF hardware is reliable. Each of the individual components are discussed below, followed by a proposed new electrode design.

- Power supply. The power supply was quite stable throughout most of the test program. There was a problem of erratic currents and voltages at the end of the test program, but this was a result of operating near the capacity level of the device. For most of the test program, a current of 0.107 mA/m^2 (0.01 mA/ft^2) was sufficient to sustain a field strength of 2.5 kV/cm. Although there was no evidence of sparking from the center wire electrode, it would still be advisable to have control circuitry on the power supply to minimize sparking.

- Electrode cable. The stainless steel electrode cable functioned well throughout the program. It is probably necessary to use stainless steel cable to ensure a long electrode life in the acid environment in a baghouse.

- Cable insulators. Even though they served the purpose, the insulator cables used in the Cherry Point electrodes were rather crude. A better design would use 0.635-cm-diameter resin rods (0.25 in.) into which the tip of the electrode cable could be fastened.

- High voltage lead. The connector from the power supply to the electrode assembly required special consideration because the acid environment in the baghouse would have destroyed the silicon rubber insulation on the wire. For this study, Teflon® tubing was used as a sheath around the high-voltage wire. This tubing also protected the wire from abrasion

where it passed through the bag cap. In a commercial installation, it would be advisable to use wire with Teflon insulation.

The attachment of the high-voltage lead to the electrode also proved to be cumbersome. With proper design, this task could be greatly simplified. One possible design would have simple connectors on each end of the high-voltage lead. One end would connect to the electrode and the other would connect to the bus from the power supply.

- Springs. The steel springs used at the pilot plant functioned quite well throughout the program with no visible signs of wear. A spring constant of 2.5 lb/in. proved easy to work with and provided sufficient tension on the electrode.

- Connectors. There were two types of connectors used in the electrode assembly: cable connectors and a high-voltage connector. The high-voltage connector was discussed earlier. The cable connectors were used to join the electrode cable with the insulating cable. Although they worked satisfactorily for the duration of the test program, the need for these connectors can be eliminated entirely in a different design. This will be illustrated in the new design described in the following text.

- Restraining bar. The restraining bars used in this study were made from scrap pieces of 1-inch angle iron with slots cut 8 inches apart to slide it onto the thimble. A small hole was drilled midway between the slots to hold a hook attached to the electrode assembly. This design worked well because the slots in the bar ensured that the lower end of the electrode assembly was always centered in the thimble. The only modification that should be made to this design is to use a piece of flat bar instead of the angle iron.

Overall, the advanced ESFF hardware used in the pilot plant worked very well, however, there is room for improvement. Specifically, the electrode design can be improved to make it easier to assemble and install. One proposed design is shown in Figure 23. The proposed design would use solid resin rods to isolate the electrode cable electrically from the bag cap and tubesheet. The resin rods would be drilled and tapped on each end to simplify the mechanical connections to the bag cap, electrode cable, spring, and restraining bar. A Teflon-insulated high-voltage cable would pass through the bag cap. At one end, this cable would be connected to the power bus. At the other end, a ceramic electrical connector would match with another ceramic connector from the electrode cable.

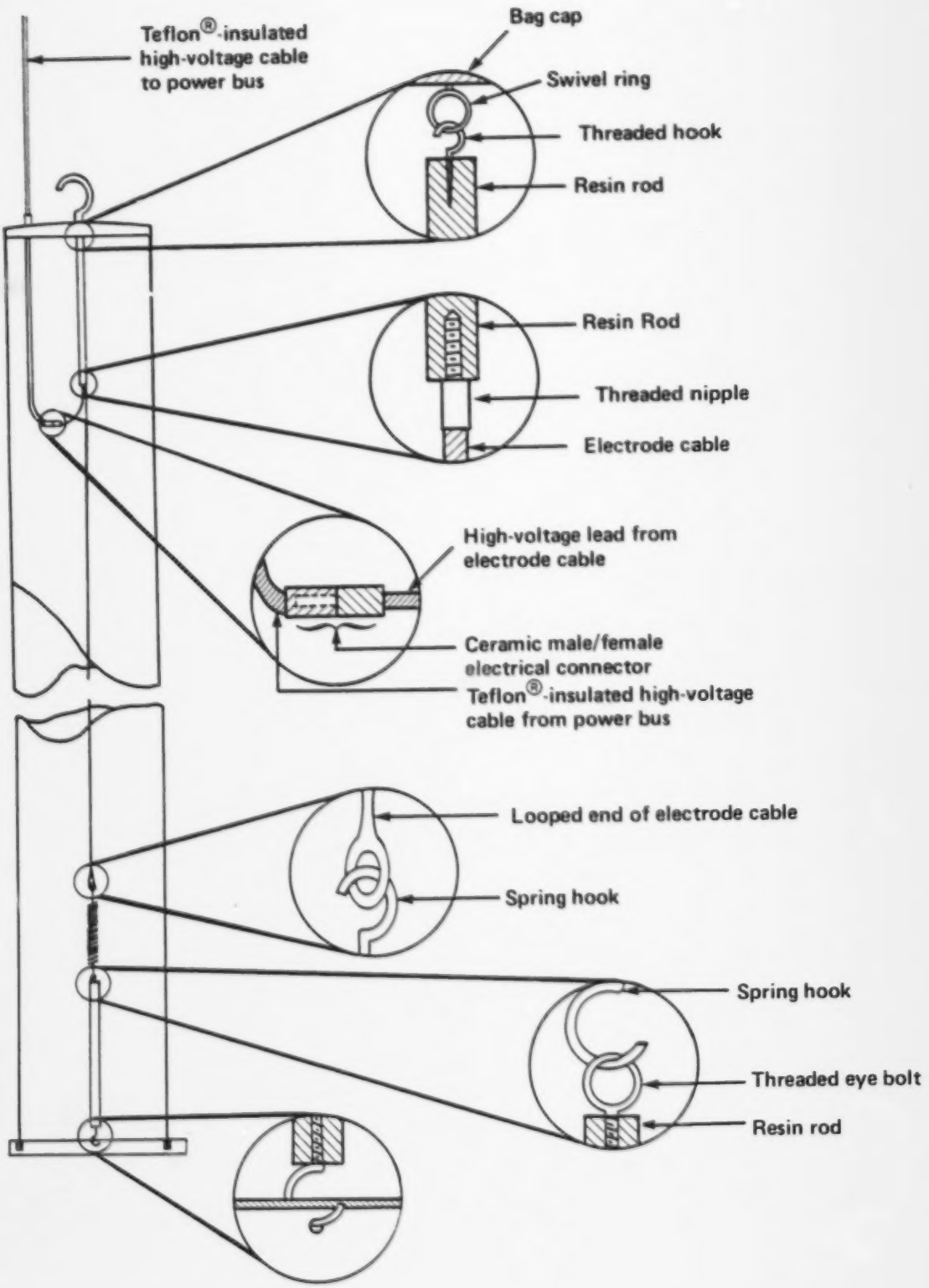

Figure 23. An improved electrode design.

This design or some variation thereof would be easy to manufacture and assemble. Also, using the ceramic connectors to link the high-voltage cable with the electrode cable would maximize ease in installation.

FUTURE WORK

The overwhelming indication of the test program results is that the advanced ESFF technology is both technically and economically feasible. However, some questions do remain. The most important question concerns the long-term stability of ESFF; that is, whether the pressure drop reduction that has been demonstrated in short-term tests persists throughout the life of a bag. This question can be answered only by a long-term test involving many bags so that statistically valid conclusions can be drawn. The best method to obtain this data would be to install advanced ESFF in a compartment of an operating baghouse and monitor the behavior over the life of the bags. It would be essential to use the individual bag-flow monitoring technique to establish the operating characteristics of each bag. Simply monitoring the overall compartment performance would not give sufficient information to prove the effectiveness of ESFF.

Other concerns to be addressed in future work include the proper design of the electrode assembly and the importance of ash resistivity in ESFF performance. The electrode design described above should be tested and modified as needed to reach an optimal configuration. Test programs should be carried out to assess the applicability of ESFF to high resistivity ashes. The ash at Cherry Point was very conductive (low resistivity), and it is possible that the ash layer collected on the bags served as the electrical ground plane. When ashes with high resistivity are to be collected, it may be necessary to alter the surface of the filter bags to make them conductive, thereby establishing the required ground.

These and other questions could best be answered in a test program at a full-scale baghouse. The best approach would be to install ESFF with IBFM monitoring hardware in a single compartment of an operating baghouse. An equal number of conventional bags in a different compartment should be fitted with IBFM hardware to serve as a control group for the test. Regular plant staff could be trained to install the electrodes within the bags and to operate and maintain the system. The objective of the test would be to turn on the ESFF power and allow the system to run with minimum intervention for 2 years or more. Data would be analyzed regularly to evaluate

the efficacy of ESFF. Operational difficulties would be noted and corrected during regular baghouse servicing. This type of test program would greatly enhance the confidence in and acceptance of advanced ESFF.

SECTION 7

CONCLUSIONS AND RECOMMENDATIONS

1. The electric field established between the center wire-electrode and the bag surface significantly reduced the rate of pressure rise in the bags. On average, the specific resistance of the ESFF bags was 70 percent less than that of the conventional bags. There were not sufficient data to determine whether the presence of electrodes woven into the fabric of one of the ESFF bags improved the electric field or affected the pressure drop characteristics.

2. The ESFF effect was clearly demonstrated by the shift in flow between electrified and nonelectrified bags when the voltage was switched from one set of bags to the other.

3. The individual bag-flow monitoring (IBFM) system worked well and was essential to the success of the program. By incorporating both conventional and ESFF bags in a single compartment, it was ensured that the two sets of bags were exposed to identical conditions.

4. The automated data acquisition and analysis system worked well and permitted unattended operation of the pilot plant for several days. The system was easy to assemble from readily available components. The amount of programming required was kept to a minimum by using commercially available software for data analysis and graphing. This system did not eliminate the need for periodic onsite inspections of the pilot plant. Random, uncontrollable events, such as boiler outages, power failures, and lightning strikes, required that an operator visit the site regularly.

5. A preliminary economic analysis of industrial-scale baghouses shows that the cost of an ESFF baghouse will be less than that of a conventional baghouse due to its smaller size. The additional cost of ESFF hardware is more than offset by the savings resulting from the smaller baghouse. The capital cost of an ESFF baghouse operated at an air-to-cloth ratio of 1.22 m/min would be 26 percent less than that of a conventional baghouse at 0.61 m/min.

6. Estimates of ESFF operating costs were found to be dependent on the stable values of fabric residual drag. Annual operating cost savings of 30 percent are predicted if residual drag proves to be 50 percent of that experienced with conventional bags.

7. Problems with the cleaning hardware significantly affected the conditions within the top-inlet compartment over a long period. Although the acceptable data present top-inlet performance as unfavorable, the limited amount of such data precludes any valid conclusions at this time.

8. A longer test interval--ideally for the life of a bag set--is necessary to judge the long-term effect of advanced ESFF on specific resistance, residual drag, and bag life.

9. A more highly automated data acquisition and analysis system would provide a more detailed account of equipment status. In addition, control circuitry could be added so that offsite engineers could easily modify experimental conditions.

SECTION 8

REFERENCES

1. Felix, L.G., and J.D. McCain. APITRON Electrostatically Augmented Fabric Filter Evaluation, EPA-600/7-79-070 (NTIS No. PB294716), February 1979.

2. Miller, B., et al. Studies of Dust Cake Formation and Structure in Fabric Filtration, EPA-600/9-81-023 (NTIS No. PB86-259986), August 1983.

3. VanOsdell, D.W., et. al. Electrostatic Augmentation of Fabric Filtration: Pulse-Jet Unit Experience, EPA-600/7-82-062 (NTIS No. PB83-16825), November 1982.

4. VanOsdell, D.W., and D.F. Furlong. Electrostatic Augmentation of Fabric Filtration: Reverse-Air Pilot Unit Experience, EPA-600/7-84-085 (NTIS No. PB84-230002), August 1984.

5. Chambers, R.L., J.J. Spivey, and D.L. Harmon. ESFF pilot plant operation at Harrington Station, in Proceedings: Fifth Symposium on the Transfer and Utilization of Particulate Control Technology, Volume 3, EPA-600/9-86-008c (NTIS No. PB86-167178), February 1986.

6. Jensen, R.M. Top inlet versus bottom inlet design, in proceedings: Fourth Symposium on the Transfer and Utilization of Particulate Control Technology, Volume I, Fabric Filtration, EPA-600/9-84-025a (NTIS No. PB85-161891), November 1984.

7. Greiner, G.P., and D.F. Furlong. Top inlet baghouse evaluation at pilot scale, presented at: Fifth Symposium on the Transfer and Utilization of Particulate Control Technology, Kansas City, MO, August 1984.

APPENDIX

DATA QUALITY ASSESSMENT

APPENDIX

DATA QUALITY ASSESSMENT

ASSESSMENT OF DATA QUALITY

In accordance with EPA guidelines, a Quality Assurance Project Plan (QAPP) was drawn up to establish goals for precision, accuracy, and completeness of the data. These Data Quality Objectives (DQOs) are outlined in Table 4, which is taken directly from the QAPP. The levels of precision, accuracy, and completeness that were actually achieved are summarized in Table 5.

DISCUSSION

All of the goals for precision and accuracy that were set forth in Table 4 were achieved at the pilot plant (Table 5), with one exception. The one deviation from the goals was due to the calibration drift of pressure transducer P9 between April 11 and July 17. This error was corrected at the time it was detected by recalibrating the transducer. The reading from the transducer was used as a redundant measurement of air flow into one of the compartments, so the loss of accuracy was not critical.

The reference method for temperature measurement was changed from that listed in the QAPP. A bimetallic thermometer was used to calibrate the thermocouple measurements at the high temperatures that are characteristic of this study (250-300 °F).

The goals for completeness were achieved except in the case of the pressure drop measurements and the electrode current. The failure to meet the completeness objective for the pressure measurements was due to computer failure, coupled with the failure of the onsite data logger. The amount of data lost would not affect the results of this study significantly. Although the electrode current was listed as a critical parameter, it is only important as an indicator of electrode performance, which was also being monitored through the electrode voltage. For this reason, the current signal was not connected to the data logger until the test program

TABLE 4. SUMMARY OF PRECISION, ACCURACY, AND COMPLETENESS OBJECTIVES

Measurement parameter	Reference	Experimental conditions	Precision	Accuracy (%)	Completeness (%)
Pressure drop	Inclined manometer	Steady state	CV=5%	5	95
Temperature	Mercury thermometer	Steady state	CV=5%	10	90
Electrode voltage	Voltmeter	Steady state	CV=10%	5	90
Electrode current	Ammeter	Steady state	CV=10%	5	90
Dust concentration	EPA Method 5	Steady state	CV=5%	10	95

CV: Coefficient of variation = (standard deviation x 100%)/mean

TABLE 5. PRECISION AND ACCURACY DATA

Measurement	Transducer No.	Test date	Typical measurement[a]	Precision (%)		Accuracy (%)		Completeness (%)
				Absolute	CV[a]	Absolute	Relative[b]	
Pressure drop (in. H_2O)	P1	5/1/85	0.1	0.0036	0.36	0.0016	0.16	92
		7/16/85	0.1	0.0038	0.38	0.0030	0.3	
	P2	5/1/85	0.1	0.0002	0.02	0.0005	0.05	92
		7/16/85	0.1	0.0039	0.39	0.0055	0.55	
	P3	5/1/85	0.1	0.002	0.2	0.0010	0.1	92
		7/16/85	0.1	0.0040	0.4	0.0006	0.06	
	P4	5/1/85	0.1	0.0021	0.21	0.0010	0.1	92
		7/16/85	0.1	0.0040	0.4	0.0007	0.07	
	P5	5/1/85	0.1	0.0021	0.21	0.0007	0.07	92
		7/16/85	0.1	0.0040	0.4	0.0022	0.22	
	P6	5/1/85	0.1	0.0012	0.22	0.0025	0.25	92
		7/16/85	0.1	0.0038	0.38	0.0032	0.32	
	P7	5/1/85	1.0	0.0006	0.006	0.0015	0.15	92
		7/16/85	1.0	0.0039	0.039	0.0021	0.21	
	P8	5/1/85	1.0	0.0026	0.026	0.0006	0.06	92
		7/16/85	1.0	0.0038	0.038	0.0010	0.10	
	P9	4/11/85	1.0	0.0012	0.12	0.004	0.4	92
		7/17/85	1.0	0.0060	0.60	0.136	13.6	
	P10	4/11/85	1.0	0.0031	0.31	0.0125	1.25	92
		7/17/85	1.0	0.0041	0.41	0.0031	0.31	
	P11	4/11/85	2.0	0.01	0.50	0.01	0.50	92
		7/17/85	2.0	0.0925	4.62	0.025	1.25	
	P12	4/11/85	2.0	0.10	5.0	0.10	5.0	92
		7/17/85	2.0	0.10	5.0	0.10	5.0	
Temperature (degrees F)	T1	6/5/85	280 (740 R)	1.0	0.013[c]	1.0	0.013[c]	92
		7/19/85	280	3.0	0.40	1.0	0.013	
	T2	6/5/85	320 (780 R)	1.0	0.013	1.0	0.013	92
		7/19/85	320	3.0	0.038	1.0	0.013	
	T3	6/5/85	275 (735 R)	1.0	0.014	1.0	0.014	92
		7/19/85	275	4.0	0.054	1.0	0.014	
	T4	6/5/85	320 (780 R)	1.0	0.013	1.0	0.013	92
		7/19/85	320	3.0	0.038	1.0	0.013	

See footnotes at end of table.

(continued)

TABLE 5 (continued)

Measurement	Transducer No.	Test date	Typical measurement[a]	Precision (%) Absolute	Precision (%) CV[a]	Accuracy (%) Absolute	Accuracy (%) Relative[b]	Completeness (%)
Electrode voltage	V1	8/5/85	25 kV	0.05 kV	0.2	0.1	0.4	92
Electrode current	C1	7/19/85	1 mA	0.05 mA	5	0.01	1	66
Dust concentration								
Gas volume		Calibrated semiannually			E%		5	100
Dust mass			20 mg	0.01 mg	0.05	0.01	0.05	

[a]Coefficient of variation is calculated as:

$$CV = \frac{\text{precision}}{\text{typical measurement}} \times 100\%$$

[b]Relative accuracy is: $\frac{\text{accuracy}}{\text{typical measurement}} \times 100\%$.

[c]Coefficient of variation and relative accuracy are computed on the basis of temperature in degrees Rankine (i.e., degrees Fahrenheit + 460).

was well underway. Also, the missing data for electrode current are from the early cycles of the study when the electrode current was quite stable (Figure 18). In summary, for the purposes of this Category 3 project, the completeness achievements were satisfactory.